

The nonorientable genus of complete tripartite graphs

M.N. Ellingham^{a,1}, Chris Stephens^{b,2}, Xiaoya Zha^{b,3}

^a Department of Mathematics, 1326 Stevenson Center, Vanderbilt University, Nashville, TN 37240, USA

^b Department of Mathematical Sciences, Middle Tennessee State University, Murfreesboro, TN 37132, USA

Received 16 October 2003

Available online 9 December 2005

Abstract

In 1976, Stahl and White conjectured that the nonorientable genus of $K_{l,m,n}$, where $l \geq m \geq n$, is $\lceil (l-2)(m+n-2)/2 \rceil$. The authors recently showed that the graphs $K_{3,3,3}$, $K_{4,4,1}$, and $K_{4,4,3}$ are counterexamples to this conjecture. Here we prove that apart from these three exceptions, the conjecture is true. In the course of the paper we introduce a construction called a transition graph, which is closely related to voltage graphs.

© 2005 Elsevier Inc. All rights reserved.

Keywords: Complete tripartite graph; Graph embedding; Nonorientable genus

1. Introduction

In this paper surfaces are compact 2-manifolds without boundary. The *orientable surface of genus h* , denoted S_h , is the sphere with h handles added, where $h \geq 0$. The *nonorientable surface of genus k* , denoted N_k , is the sphere with k crosscaps added, where $k \geq 1$. A graph is said to be *embeddable* on a surface if it can be drawn on that surface in such a way that no two edges cross. Such a drawing is referred to as an *embedding*. The *genus* $g(G)$ of the graph G is the minimum h such that G can be embedded on S_h . Likewise the *nonorientable genus* $\tilde{g}(G)$ of G is the minimum k such that G can be embedded on N_k . For convenience, we define

E-mail addresses: mne@math.vanderbilt.edu (M.N. Ellingham), cstephen@mtsu.edu (C. Stephens), xzha@mtsu.edu (X. Zha).

¹ Supported by NSF Grants DMS-0070613 and DMS-0215442.

² Supported by NSF Grant DMS-0070613 and Vanderbilt University's College of Arts and Sciences Summer Research Award.

³ Supported by NSF Grant DMS-0070430.

the nonorientable genus of a planar graph to be zero. An embedding of G on $S_{g(G)}$ is called a *minimal embedding* for G , and one on $N_{\tilde{g}(G)}$ is called a *minimal nonorientable embedding*.

The problem of determining the genus of a graph, like many other problems in graph theory, began in connection with the four-color problem. In 1890, Heawood [10] proposed a generalization of the four-color conjecture to higher surfaces. He defined the chromatic number of a surface to be the maximum chromatic number over all graphs embeddable in that surface. He then calculated an upper bound for the chromatic number of a nonplanar surface, namely $\chi(\Sigma) \leq \lfloor (7 + \sqrt{49 - 24c})/2 \rfloor$, where c is the Euler characteristic of Σ , and conjectured that each surface attained this lower bound.

Heawood's conjecture for orientable surfaces was implied by the conjecture that the minimum genus of the complete graph K_n is $\lceil (n-3)(n-4)/12 \rceil$. In 1891, Heffter [11] proved it true for all $n \leq 12$ and for the numbers n of the form $n = 12s + 7$ where $q = 4s + 3$ is a prime number and the order of the element 2 in the multiplicative group of integers (mod q) is either $q - 1$ or $(q - 1)/2$. After this very little progress was made on Heawood's conjecture until 1952, when Ringel proved that it is true for $n = 13$, and then 1954, when he proved it true for all $n \equiv 5 \pmod{12}$ [18,19]. During the 1960s several authors contributed other cases (see [22]). The problem was finally settled in 1968 by Ringel and Youngs [23], and the solution of the problem helped to establish topological graph theory as a major research area. The corresponding nonorientable problem, that the minimal nonorientable genus of K_n is $\lceil (n-3)(n-4)/6 \rceil$, was solved in 1954 by Ringel [18], with one exception: the nonorientable genus of K_7 is 3 rather than the expected 2 [8]. For a thorough discussion of the Heawood problem and its solution, see [22].

A related result from this period was Ringel's 1965 solution of the genus problem for complete bipartite graphs [20,21]. He proved that the genus of $K_{m,n}$ is $\lceil (m-2)(n-2)/4 \rceil$, and the nonorientable genus of $K_{m,n}$ is $\lceil (m-2)(n-2)/2 \rceil$. One natural extension of this result would be to complete tripartite graphs. Equation (1) of the following conjecture was proposed by White [26]. Equation (2) was proposed by Stahl and White [25].

Conjecture 1. [25,26] *The orientable genus of $K_{l,m,n}$, where $l \geq m \geq n$, is*

$$g(K_{l,m,n}) = \left\lceil \frac{(l-2)(m+n-2)}{4} \right\rceil, \quad (1)$$

and its nonorientable genus is

$$\tilde{g}(K_{l,m,n}) = \left\lceil \frac{(l-2)(m+n-2)}{2} \right\rceil. \quad (2)$$

One observes that the conjectured value of the genus (respectively nonorientable genus) of $K_{l,m,n}$ is the same as the known value for the genus (respectively nonorientable genus) of $K_{l,m+n}$. In other words, Conjecture 1 claims that there exists a minimal embedding and a minimal nonorientable embedding of $K_{l,m+n}$, each with enough "room" in the embedding to add edges which would transform $K_{l,m+n}$ into $K_{l,m,n}$. Unfortunately, the known minimal embeddings for the complete bipartite graphs do not seem to have this property.

Ringel and Youngs [24] proved (1) true for $K_{n,n,n}$. White proved that (1) is true for $K_{l,m,n}$ where $m+n \leq 6$ [26], and for $K_{mn,n,n}$, where $m, n \in \mathbb{N}$ [27]. Stahl and White [25] proved that (1) holds for $K_{n,n,n-2}$ when $n \geq 2$ is even, and for $K_{2n,2n,n}$ for all $n \geq 1$. They also showed that (2) holds for $K_{n,n,n-2}$ when $n \geq 2$, and for $K_{n,n,n-4}$ when $n \geq 4$ is even.

In 1991, Craft [4,5] used surgical techniques to prove (1) true if $m + n$ is even and $l \geq 2m$. He also showed that if $m + n$ is odd and p is the smallest integer which is at least $m/2$ and such that $p + n \equiv 2 \pmod{4}$, then (1) is true provided $l \geq 4 \max\{p, n\} + 2$.

Recently, the authors [7] showed that in fact (2) is not true for $K_{3,3,3}$, $K_{4,4,1}$, or $K_{4,4,3}$. They also showed that these are the only counterexamples with $l \leq 5$ to either case of the conjecture.

In this paper we solve the nonorientable genus problem for $K_{l,m,n}$. The general idea of the proof is as follows. First, we use a surgical technique we call the “diamond sum” to reduce the general case $K_{l,m,n}$ to the semisymmetric case $K_{m,m,n}$. Second, we delete the smallest set of the tripartition and try to find an embedding of the bipartite graph $K_{m,m}$ with n large faces, observing that afterwards we may put the n vertices back into the embedding by placing one vertex in each of the n large faces. Third, we use a construction called the “transition graph” to find the appropriate embedding of $K_{m,m}$. Because of limitations of the diamond sum, these techniques do not work in every case; for some m and n we must also deal separately with the nonsymmetric case $K_{m+1,m,n}$.

Section 2 contains notation and terminology and a brief explanation of the diamond sum technique. Section 3 provides definitions and some preliminary theory for the transition graph construction. In Section 4 we prove the main theorem, and finally in Section 5 we suggest some areas for further research.

2. Preliminaries

In this section we lay out the necessary definitions and then briefly explain our main surgical technique.

2.1. Notation and terminology

For background in topological graph theory see [9] or [16].

As previously mentioned, an embedding of a graph on a surface is a drawing of that graph on that surface in such a way that no two edges cross. If a graph is embedded in such a way that each face is homeomorphic to an open disk in the plane, then the embedding may be completely described combinatorially using *local rotations* and *edge signatures*. A local rotation π_v at the vertex v is a cyclic permutation of the edges incident with v . An edge signature is a mapping λ from the edges of a graph into $\{-1, 1\}$.

If an embedding is given entirely in terms of local rotations and edge signatures, we may calculate the orientability of the embedding surface in the following way. An embedding is nonorientable if and only if there is some closed walk in the embedded graph which encounters an odd number of edges of signature -1 .

2.2. The diamond sum

Here we describe our reduction technique, from [14]. The construction, in a different form, was introduced by Bouchet [2], who used it to obtain a new proof of Ringel’s 1965 result [20,21] on the genera of complete bipartite graphs. A reinterpretation of Bouchet’s construction appeared in a paper by Magajna et al. [15], and was described more fully by Mohar et al. [17].

Suppose $\psi_1: G_1 \rightarrow \Sigma_1$ is an embedding of G_1 on the surface Σ_1 and $\psi_2: G_2 \rightarrow \Sigma_2$ is an embedding of G_2 on the surface Σ_2 . G_1 and G_2 may have loops or multiple edges. Moreover,

suppose that there exist vertices u in G_1 and v in G_2 , neither incident with any loops or multiple edges, where u has n neighbors u_0, \dots, u_{n-1} , in this (local) clockwise order, and v has n neighbors v_{n-1}, \dots, v_0 , in this clockwise order. Let D_1 be a closed disk contained in a small neighborhood of $\text{st}(u) = \{u\} \cup \{uu_0, \dots, uu_{n-1}\}$ that contains $\text{st}(u)$ and intersects G only at u_0, \dots, u_{n-1} . Define the closed disk D_2 containing $\text{st}(v)$ in a similar way. Remove the interiors of D_1 and D_2 from the surfaces Σ_1 and Σ_2 , respectively, and identify the boundaries of $\Sigma_1 \setminus \text{int}(D_1)$ and $\Sigma_2 \setminus \text{int}(D_2)$ in such a way that u_i is identified with v_i for all i , $0 \leq i \leq n-1$. Thus we obtain a new embedding Ψ of a new graph G into the surface $\Sigma_1 \# \Sigma_2$, where $\#$ denotes the connected sum of two surfaces. G is obtained from $G_1 \setminus \{u\}$ and $G_2 \setminus \{v\}$ by identifying u_i with v_i for all i , $0 \leq i \leq n-1$ (which may create new multiple edges). Of course the resulting graph depends on the alignment of the u_i and the v_i . However, in this paper the u_i (and likewise the v_i) end up being generic vertices from the same part of a bi- or tripartition, so we do not care about their alignment. Thus we may call the operation on the graphs a *diamond sum of graphs* (with respect to the vertices u and v), denoted $(G_1, u) \diamond (G_2, v)$, and the operation on the embeddings a *diamond sum of embeddings* (with respect to u and v), denoted $\Psi_1(G_1, u) \diamond \Psi_2(G_2, v)$.

We make the following observations about this construction. First, if one of the embeddings Ψ_1 or Ψ_2 is nonorientable, then so is the resulting embedding Ψ . Second, if we take G_1 to be $K_{l,m,n}$ and take $u \in V(G_1)$ from the part of the tripartition with l vertices, and take $G_2 = K_{k+2,m+n}$, with $v \in V(G_2)$ in the part of the bipartition that has $k+2$ vertices, then $(G_1, u) \diamond (G_2, v)$ yields the graph $G = K_{l+k,m,n}$. In this case it is often true that if Ψ_1 is an embedding of $K_{l,m,n}$ satisfying Conjecture 1, and if Ψ_2 is a minimal genus embedding of $K_{k+2,m+n}$, then Ψ is an embedding of $K_{l+k,m,n}$ satisfying Conjecture 1. The details of when this works are discussed in [14].

For the purposes of this paper, the important case is the following:

Theorem 2. [14] *If $K_{l,m,n}$ satisfies (2) from Conjecture 1 then so does $K_{l+k,m,n}$ provided that at least one of k , l , or $m+n$ is even.*

3. Transition graphs

The goal of this section is to introduce the transition graphs and to build enough of a theoretical foundation so that we can use them. Transition graphs are closely related to voltage graphs. In fact, a transition graph is really just the medial graph of an embedded voltage graph. Archdeacon [1] obtained some results by placing voltages and currents on the edges of medial graphs. Our construction differs from Archdeacon's in that our voltages do not end up on the edges of the medial graph, but the vertices (because, in a sense, the voltage assignment is performed before the medial graph is constructed). For background on voltage graphs, see [9]. In this paper we shall represent embedded voltage graphs by an ordered pair $(G \rightarrow \Sigma, \alpha)$, where $G \rightarrow \Sigma$ represents an embedding of the directed graph G on the surface Σ , and α is a voltage assignment to the directed edges of G .

Here we will include two results from [9] about voltage graphs which will be useful later. First, given an embedded voltage graph, it would be nice to calculate the Euler genus of the surface of the derived embedding without explicitly calculating the derived graph. Theorem 3 accomplishes such a calculation. Second, Theorem 4 gives a method for determining orientability of a derived embedding.

Theorem 3. [9] *Let C be the boundary walk of a face of size k in the embedded voltage graph $(G \rightarrow \Sigma, \alpha)$. If the net voltage on the closed walk C has order n in the voltage group Γ , then there are $|\Gamma|/n$ faces of the derived embedding $G^\alpha \rightarrow \Sigma^\alpha$ corresponding to the region bounded by C , each with kn sides.*

Theorem 4. [9] *Let $(G \rightarrow \Sigma, \alpha)$ be an embedded voltage graph. Then the derived surface is nonorientable if and only if there is some closed walk W in the base embedding $G \rightarrow \Sigma$ such that a traversal of W encounters an odd number of edges with -1 signature, and the net voltage on W equals the identity.*

3.1. Transition graphs

As previously mentioned, transition graphs are closely related to embedded voltage graphs (in fact, they are equivalent!). In a transition graph, though, the emphasis is slightly different. In the case of a voltage graph and its derived graph, vertices correspond to vertices and edges to edges. On the other hand, vertices of a transition graph correspond to edges of the derived graph, and edges of the transition graph correspond to consecutive pairs of edges (“transitions”) in the local rotations of the derived graph. Vertices of the derived graph do not appear directly in the transition graph; local rotations at vertices of the derived graph, though, correspond to closed trails in the transition graph.

The advantage of the transition graph is mostly visual. For instance, in the transition graphs used for the proof of the main theorem in this paper, one can determine the number and sizes of the derived faces at a glance. Contrast this situation with that of embedded voltage graphs, in which one must trace faces and compute net voltages to determine face sizes in the derived embedding. A similar state of affairs occurred in the proof of Heawood’s conjecture, where the main tools used were not embedded voltage graphs, but embedded current graphs: although the constructions are dual to one another, in the context of Heawood’s conjecture current graphs are more readily manipulated and verified than voltage graphs.

Because of the close relationship with voltage graphs, we have tried to keep the terminology similar. The reader may refer to Fig. 1 for an example of a transition graph and corresponding embedded voltage graph. The formalism follows.

Definition 5. A transition graph $\mathcal{G} = (D, \mathcal{C}, \lambda, \alpha)$ consists of the following:

- (1) a digraph D such that at each vertex both the indegree and the outdegree are equal to 2;
- (2) a collection \mathcal{C} of directed closed trails C_0, \dots, C_{n-1} partitioning $E(D)$;
- (3) at each vertex of D an ordering $C_i \rightarrow C_j$ of the two⁴ directed closed trails incident with that vertex;
- (4) a function $\lambda: \mathcal{V} \rightarrow \{-1, +1\}$;
- (5) a function α from \mathcal{V} into a (usually finite) group Γ .

We call Γ the voltage group and α the voltage assignment.

⁴ In the case that there is only one directed trail C incident with a vertex u , then C meets u twice. Suppose u is the head of e^- and f^- and u is the tail of e^+ and f^+ , where e^-, e^+ are consecutive edges of C , and f^-, f^+ are consecutive edges of C (and possibly $e^- = f^+$ or $e^+ = f^-$). Then at u we fix an ordering, without loss of generality $\{e^-, e^+\} \rightarrow \{f^-, f^+\}$.

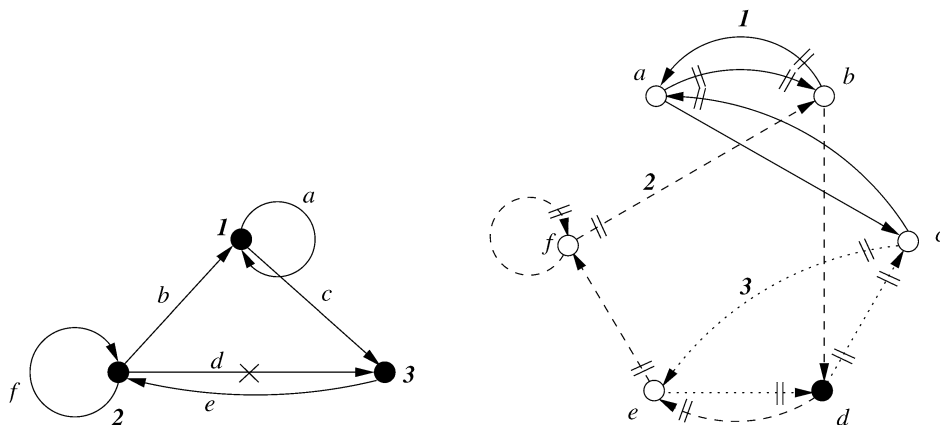


Fig. 1. An embedded voltage graph and corresponding transition graph. Double slash marks through a cycle C_0 near a vertex u (incident with trails C_0 and C_1) are used to signify that $C_1 \rightarrow C_0$ at u ; at vertices incident with only one trail, the double slashes also determine which edges are to be paired. The 'x' on edge d and the solid coloring of vertex d represents a signature of -1 .

While we may obtain a derived embedding directly from a transition graph, it may be more helpful to explain instead how to get back to the corresponding embedded voltage graph. The embedded voltage graph $(H \rightarrow \Sigma, \beta)$ that corresponds to a given transition graph $\mathcal{G} = (D, \mathcal{C}, \lambda, \alpha)$, has one vertex v_j for each directed closed trail $C_j \in \mathcal{C}$, and one edge e_i for each vertex $u_i \in D$. Incidence in the voltage graph is calculated in the following way. If the vertex $u_i \in V(D)$ is incident with the two directed closed trails C_j and C_k , where $C_j \rightarrow C_k$ is the ordering of the trails at u_i , then the edge e_i runs from v_j to v_k in the voltage graph. If $u_i \in V(D)$ is incident with only the directed trail C_j , then the corresponding edge $e_i \in V(H)$ is a loop at $v_j \in V(H)$. The voltage $\beta(e_i)$ in the voltage graph is the same as the voltage $\alpha(u_i)$ in the transition graph. The edge signature of e_i in H is just $\lambda(u_i)$. If $C_i = u_{i_0}u_{i_1} \dots u_{i_{l-1}}$ in \mathcal{G} , then the local rotation at $v_i \in V(H)$ is $(e_{i_0}e_{i_1} \dots e_{i_{l-1}})$. (See Fig. 1.)

If we want to recover the faces of a derived embedding of a transition graph, we may reword Theorem 3 in the language of transition graphs. We calculate the *boundary walks* of a transition graph $\mathcal{G} = (D, \mathcal{C}, \lambda, \alpha)$ by the *boundary traversal procedure*: Start by walking along a forward edge $e = u_i \rightarrow u_j$ in D . Next, there are two forward edges leaving u_j ; take the one that is not in the same directed trail of \mathcal{C} as e . (If u_j is incident with only one directed trail of \mathcal{C} , then take the forward edge leaving u_j which is not linked with e .) Continue in this manner until e is reached once more, with the following exception. If a vertex $u_k \in V(D)$ is encountered with $\lambda(u_k) = -1$, then begin traversing edges in the negative direction until another -1 signature is encountered. The resulting walk is called a *boundary walk* of the transition graph, and each directed edge of the transition graph is in exactly one boundary walk (possibly up to reversal). Also, each vertex of the transition graph is in at most two boundary walks (corresponding to the fact that each edge of an embedded voltage graph is in at most two faces).

The *net transition* on a boundary walk

$$W = e_{j_0}u_{i_0}e_{j_1}u_{i_1} \dots e_{j_{l-1}}u_{i_{l-1}}e_{j_0}$$

is

$$\alpha(u_{i_0})^{\epsilon_0} \cdot \alpha(u_{i_1})^{\epsilon_1} \dots \alpha(u_{i_{l-1}})^{\epsilon_{l-1}},$$

where ϵ_j is calculated in the following way. If e_{j_k} and $e_{j_{k+1}}$ are in directed trails C_a and C_b , respectively, and if at u_k the trails are ordered $C_a \rightarrow C_b$, then $\epsilon_k = +1$. If the trails are ordered $C_b \rightarrow C_a$, then $\epsilon_k = -1$. If there is only one directed trail incident with u_{i_k} , then e_{j_k} is either a member of the “head” pair or the “tail” pair of edges at u_{i_k} . If the latter, then $\epsilon_k = +1$; if the former, then $\epsilon_k = -1$.

Theorem 6. *Let F be a boundary walk of size k in the transition graph \mathcal{G} . If the net voltage on the closed walk F has order n in the voltage group Γ , then there are $|\Gamma|/n$ faces of the derived embedding $G^\alpha \rightarrow \Sigma^\alpha$ corresponding to the region bounded by F , each with kn sides.*

3.2. Transition graphs for minimal embeddings of $K_{l,m,n}$

All the voltage graphs that we need in the proof of our main theorem are loopless two-vertex voltage graphs with all edges directed from left to right. The two vertices correspond to the two parts of a bipartition of $K_{m,m}$. Moreover, all our voltage groups are cyclic groups \mathbb{Z}_m , and every voltage occurs exactly once. In the derived graph, therefore, every vertex in one part of the partition is joined to every vertex in the other part of the partition. Thus we can eliminate much of the generality found in the previous section.

First, let us establish a notational convenience. Since our voltage graphs have no loops, all directed trails are in fact directed cycles. (A directed trail of a transition graph corresponds to a local rotation about a vertex of an embedded voltage graph, and a vertex of a transition graph corresponds to an edge of a voltage graph. The only way a local rotation can contain the same edge twice is for that edge to be a loop.) Also, since all our voltage graphs contain two vertices, their corresponding transition graphs each contain exactly two cycles. In the future, let us therefore agree that such transition graphs should each have one cycle depicted with solid edges, and one cycle depicted by dashed edges. Moreover, since all edges of the voltage graph are directed from left to right, let us adopt the convention that the ordering in the transition graphs with $n = 2$ is always from solid to dashed. Let us also agree to draw the vertex v_i solid if $\lambda(v_i) = -1$ and open otherwise. Finally, since all our voltage groups are cyclic and our voltage assignments bijective, we shall find it most helpful to draw the vertices of the transition graphs in a circular pattern, with the voltage assignments increasing by increments of one as the vertices are followed in the clockwise direction. (See Fig. 2.) If a transition graph (with cyclic voltage group \mathbb{Z}_m of order m

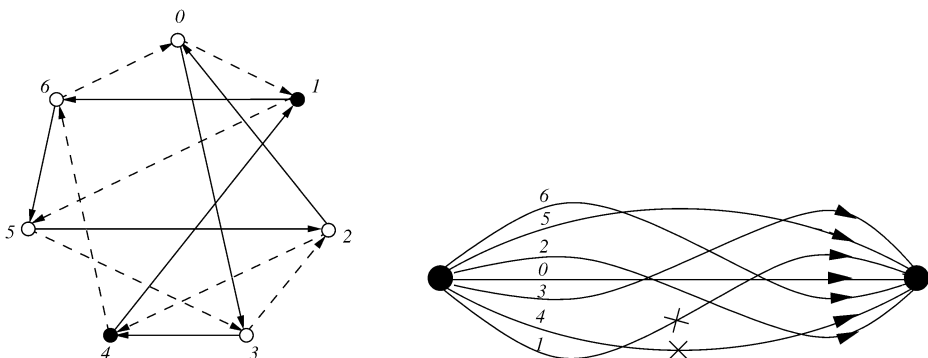


Fig. 2. A cyclic 7-transition graph and corresponding voltage graph.

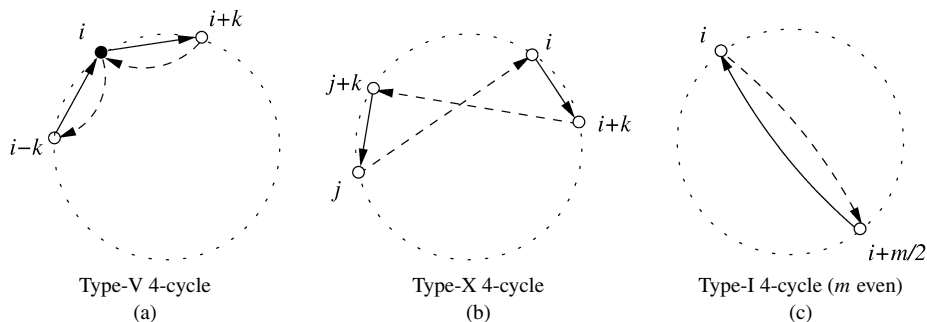


Fig. 3. Three classes of 4-cycles.

and bijective voltage assignment) is drawn in such a manner, let us call it a cyclic m -transition graph. Also, for simplicity of notation we shall simply label each vertex in a cyclic m -transition graph by its image under α .

Here we obtain some specific applications of Theorem 6.

Let \mathcal{G} be a cyclic m -transition graph. Suppose \mathcal{G} has a boundary walk $W = (i, i+k, i, i-k, i)$. Then W has net transition 0 and length 4, and therefore corresponds to m facial 4-cycles in the derived embedding. We shall denote such boundary walks “4-cycles of type V.” An example is shown in Fig. 3(a). Note that the edge orientations and the vertex signatures of a 4-cycle of type V do not necessarily have to be as in Fig. 3(a).

Now suppose \mathcal{G} has a boundary walk $W' = (i, i+k, j+k, j, i)$. Then W' has net transition 0 and length 4, and therefore corresponds to m facial 4-cycles in the derived embedding. Denote such boundary walks “4-cycles of type X.” An example is shown in Fig. 3(b). Note that the edge orientations and the vertex signatures of a 4-cycle of type X do not necessarily have to be as in Fig. 3(b).

Let m be even and let \mathcal{G} be a cyclic m -transition graph with a boundary walk $W'' = (i, i+m/2, i)$. Then W'' has net transition $m/2$ and length 2, and therefore corresponds to $m/2$ facial 4-cycles in the derived embedding. Denote such cycles “4-cycles of type I.” An example is shown in Fig. 3(c). Note that the edge orientations and the vertex signatures of a 4-cycle of type I do not necessarily have to be as in Fig. 3(c).

Finally, let \mathcal{G} be a cyclic m -transition graph with a boundary walk $F = (i, i+1, i)$. Then F has net transition 1 and length 2, and therefore corresponds to a single facial cycle of length $2m$. Call such cycles “hamilton cycles of type H.” An example is shown in Fig. 4. Note that the edge orientations and the vertex signatures of a hamilton cycle of type H do not necessarily have to be as in Fig. 4.

More generally, if \mathcal{G} is a cyclic m -transition graph with a boundary walk $F' = (i, i+k, i)$, where $\gcd(k, m) = 1$, then F' has net transition k and length 2, and therefore corresponds to a single facial cycle of length $2m$.

We have a nice analog of Theorem 4 for cyclic m -transition graphs.

Theorem 7. Let \mathcal{G} be a cyclic m -transition graph. Then the derived embedding is nonorientable if and only if there is some sequence of vertices $(n_0, n_1, \dots, n_{k-1})$, where k is even, such that an odd number of the n_i 's have $\lambda(n_i) = -1$, and $n_0 - n_1 + n_2 - n_3 + \dots - n_{k-1} = 0$ in \mathbb{Z}_m .

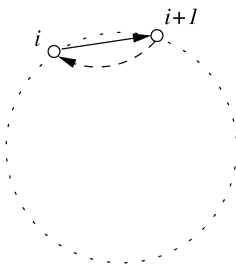


Fig. 4. A type-H hamilton cycle.

3.3. Partial transition graphs

We first need to introduce the concept of a relative embedding. Let G be a graph, and let \mathcal{F} be a collection of closed walks F_0, \dots, F_k from G such that each edge of G appears at most twice in \mathcal{F} . At each vertex x of G , construct the graph G_x in the following way. $V(G_x) = \{u_e \mid e \in E(G) \text{ and } e = xy \text{ for some } y \in V(G)\}$, and we join two vertices u_e, u_f in G_x by one edge for each $F_i \in \mathcal{F}$ containing either ef or fe as a subwalk. If for all $x \in V(G)$, the graph G_x contains no cycle which is not spanning, then we call \mathcal{F} a *relative embedding*.

In some of the cases in the proof of our main theorem, our embeddings are not symmetric enough to be completely described using transition graphs, but they do possess enough symmetry to be “almost” completely described by transition graphs. In these cases, we use “partial” transition graphs; i.e., transition graphs missing a few edges. They are, as usual, (partial) cyclic m -transition graphs. Instead of containing a solid and a dashed cycle, partial (cyclic) transition graphs contain some solid paths, and some dashed paths, representing partial local rotations at each derived vertex. Thus, while transition graphs give rise to derived embeddings, partial transition graphs give rise to derived relative embeddings.

Definition 8. A *partial transition graph* $\mathcal{G} = (D, \mathcal{C}, \lambda, \alpha)$ consists of the following:

- (1) a digraph D such that at each vertex both the indegree and the outdegree are at most 2;
- (2) a collection $\mathcal{C} = \{C_0, \dots, C_{n-1}\}$ such that each C_i is a “partial directed closed trail”, i.e., a set of pairwise vertex-disjoint directed trails, and the C_i partition $E(D)$;
- (3) at each $v \in V(D)$ such that $d^+(v) = d^-(v) = 2$ an ordering $C_i \rightarrow C_j$ of the two (see footnote 4) directed closed trails incident with that vertex;
- (4) a function $\lambda: \mathcal{V} \rightarrow \{-1, +1\}$, together with the following restrictions: if $\lambda(v) = +1$, then $d^+(v) = d^-(v)$; if $\lambda(v) = -1$ then both $d^+(v)$ and $d^-(v)$ are even;
- (5) a function α from \mathcal{V} into a (usually finite) group Γ .

When we construct part of an embedding using partial transition graphs, we still need to know something about the orientability of the embedding. In this case, we need a slightly weaker hypothesis than that in Theorem 7, and we are willing to accept a weaker conclusion. We use the following.

Theorem 9. Let \mathcal{G} be a partial cyclic m -transition graph. Suppose that there is some sequence of vertices $(n_0, n_1, \dots, n_{k-1})$, where k is even, such that an odd number of the n_i 's have $\lambda(n_i) = -1$, $n_0 - n_1 + n_2 - n_3 + \dots - n_{k-1} = 0$, and for each $0 \leq i \leq k-1$, n_i and n_{i+1} are in the

same component of one of the partial directed closed trails C_j . Then the relative embedding represented by \mathcal{G} is nonorientable.

The theorem is true because the hypotheses guarantee that we can find an orientation-reversing path in the derived relative embedding. That is, in the derived embedding there is a closed walk with an odd number of edges of signature -1 . We omit the details.

4. Main result

We are now prepared to prove the main theorem:

Theorem 10. *The nonorientable genus of the complete tripartite graph $K_{l,m,n}$, where $l \geq m \geq n$, is $\lceil (l-2)(m+n-2)/2 \rceil$, except for $K_{3,3,3}$, $K_{4,4,1}$, and $K_{4,4,3}$, each of which has nonorientable genus $\lceil (l-2)(m+n-2)/2 \rceil + 1$.*

Proof. The exceptional cases $K_{3,3,3}$, $K_{4,4,1}$, and $K_{4,4,3}$ were handled in [7]. For the rest, the proof is by induction on l , using Theorem 2. Thus it suffices to establish (2) from Conjecture 1 for $K_{m,m,n}$ when m and n have the same parity (Case I); for $K_{m,m,n}$ when m is even and n is odd (Case III); and for both $K_{m,m,n}$ and $K_{m+1,m,n}$ when m is odd and n is even (Case II).

We divide Case I into two subcases, namely the subcase that $m > n$ and the subcase that $m = n$. In Case II we separate into three subcases: $K_{m,m,n}$ for $n \geq 4$; $K_{m,m,n}$ for $n = 2$; and $K_{m+1,m,n}$. Finally, we divide Case III into three subcases: $m \equiv 2 \pmod{4}$; $m \equiv 0 \pmod{4}$, $n \geq 3$; and $m \equiv 0 \pmod{4}$, $n = 1$.

4.1. Case I: m and n have the same parity

Subcase $m > n \geq 1$

Claim 11. *Theorem 10 is true for the case $m + n$ even, $m > n \geq 1$.*

Proof. Suppose $m + n$ is even, where $m > n \geq 1$. We prove the basis case $l = m$, i.e., we find the required embedding for $K_{m,m,n}$. The claim then follows for $l > m$ by Theorem 2.

Let \mathcal{G} be the cyclic m -transition graph with solid edges $i \rightarrow (i+1)$ for all values of i (modulo m), dashed edges $i \rightarrow (i-1)$ for all values of i (modulo m), and signatures of -1 on the vertices $n+1, n+3, \dots, m-1$. (See Fig. 5.) Then \mathcal{G} contains n type-H hamilton cycles and $(m-n)/2$ type-V 4-cycles, implying that the derived embedding $G^\alpha \rightarrow \Sigma^\alpha$ (where G^α is $K_{m,m}$) consists of $m(m-n)/2$ facial 4-cycles and n facial hamilton cycles. Applying Euler's formula, we see that Σ^α is a surface of genus $(m-2)(m+n-2)/2$. We see that Σ^α is nonorientable by applying Theorem 7 to the sequence of vertices $(n, n+1, n, n-1)$.

To illustrate this case in more detail, Fig. 6 depicts an embedded two-vertex voltage graph and the corresponding transition graph for the case $m = 7$, $n = 3$. The walks $(0, 1, 0, 6, 0)$ and $(5, 6, 5, 4, 5)$ are 4-cycles of type V; the walks $(1, 2, 1)$, $(2, 3, 2)$, and $(3, 4, 3)$ are hamilton cycles of type H. For convenience, if $K_{m,m}$ has bipartition $\{x_0, \dots, x_{m-1}\} \cup \{y_0, \dots, y_{m-1}\}$, let us say that an edge of the form $x_i y_{i+k}$ (subscripts mod m) has slope k . Then, for instance, the edge in the voltage graph of Fig. 6 with voltage assignment 0 corresponds to all edges of slope 0 in the derived graph. Also, the vertex of the transition graph labeled with voltage 0 corresponds to all edges of slope 0 in the derived graph. The solid edge $0 \rightarrow 1$ in the transition graph of

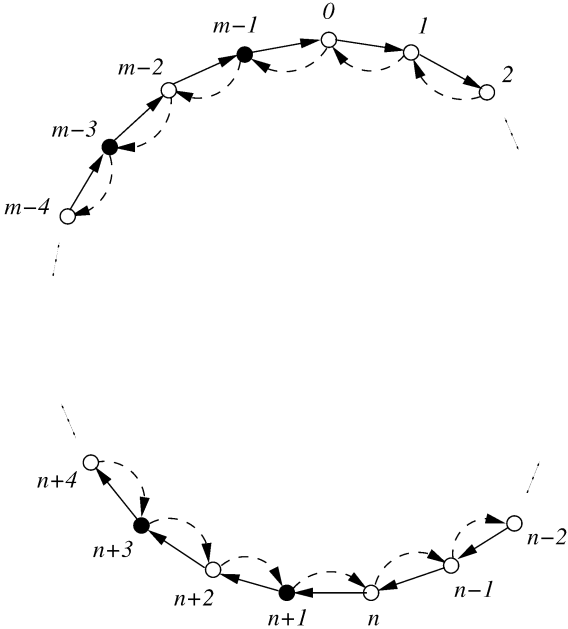


Fig. 5. Transition graph for the case $m + n$ even.

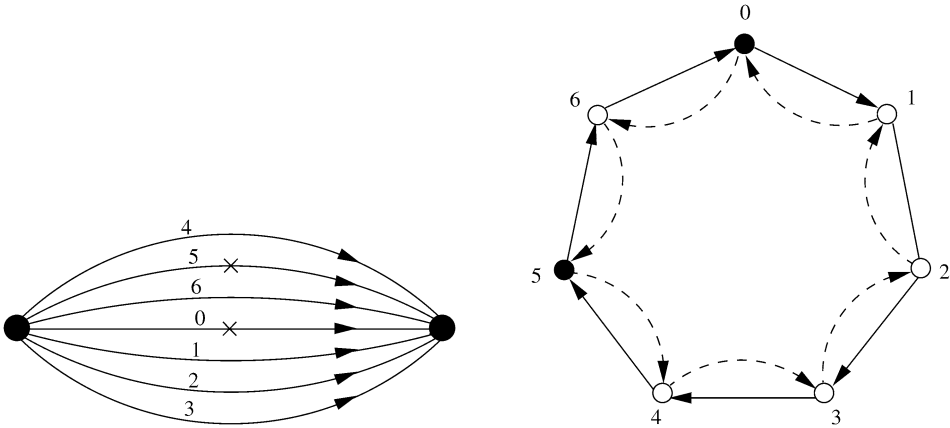


Fig. 6. An embedding of $K_{7,7}$ with 3 hamilton cycles.

Fig. 6 means that at each vertex x_i on the left side of the bipartition of the derived graph (see Fig. 7), there is a face containing both of the edges $x_i y_i$ and $x_i y_{i+1}$. The fact that $(0, 1, 0, 6, 0)$ is a boundary walk of the transition graph means that at each vertex x_i of the derived graph, there is a facial cycle $x_i y_i x_{i-1} y_{i-1} x_{i-1-6}$, where of course $x_{i-1-6} = x_i$. These particular facial cycles are shown in Fig. 7(a). Likewise the faces corresponding to the boundary walks $(5, 6, 5, 4, 5)$, $(1, 2, 1)$, $(2, 3, 2)$, and $(3, 4, 3)$ are shown in Fig. 7, parts (b)–(e), respectively.

This completes the proof of the claim. \square

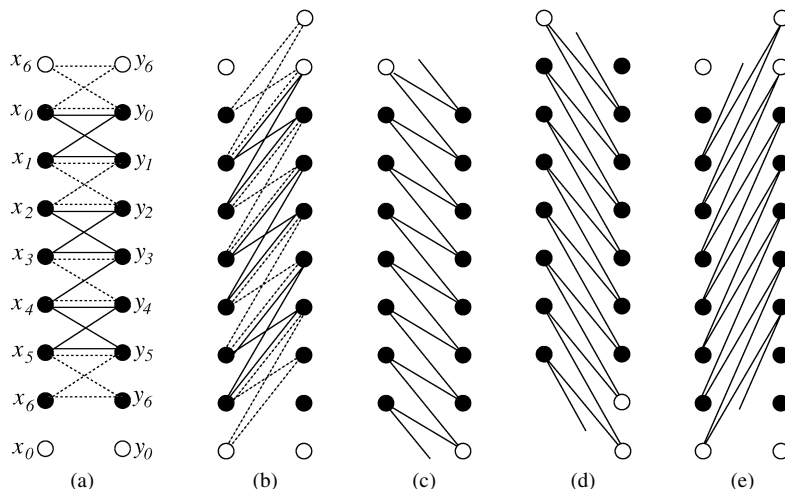


Fig. 7. The explicit faces corresponding to Fig. 6.

Subcase $m = n \geq 1$

Claim 12. Theorem 10 is true for the case $m = n \geq 1$.

Proof. We again prove the basis case $l = m$ by examining $K_{m,m,m}$, and the claim for $K_{l,m,m}$ then follows for $l > m$ by Theorem 2. $K_{1,1,1}$ and $K_{2,2,2}$ are planar. We must treat $n = 3$ as a special case. $K_{3,3,3}$ does not conform to Eq. (2) (see [7]); thus we must use $K_{4,3,3}$ as a basis case for our induction. An embedding of $K_{4,3,3}$ on N_4 can be found in [7].

For $n \geq 4$, the construction from Claim 11 with $m = n$ does give an embedding of $K_{n,n,n}$, but that embedding turns out to be orientable. A transition graph \mathcal{H} corresponding to that embedding is shown in Fig. 8(a).

To obtain the desired nonorientable embedding, we simply modify the orientable one corresponding to \mathcal{H} in the following way. First, we define the partial transition graph \mathcal{G} to be the one obtained by removing solid edges $(n-2) \rightarrow (n-1)$, $(n-1) \rightarrow 0$, $0 \rightarrow 1$, and $1 \rightarrow 2$ and removing dashed edges $2 \rightarrow 1$, $1 \rightarrow 0$, $0 \rightarrow (n-1)$, and $(n-1) \rightarrow (n-2)$ from the transition graph \mathcal{H} (see Fig. 8(b)). Next, we explicitly choose hamilton cycles in the bipartite graph $K_{n,n}$ which together use the edges with slopes 2 and $n-2$ once each and the edges with slopes $n-1$, 0, and 1 twice each. Moreover, we choose them in such a way that they cannot be given a consistent orientation. We deal with each residue class modulo 4 separately.

First, suppose $n \equiv 0 \pmod{4}$. If $n \geq 8$, Fig. 9 shows the additional facial cycles we add to the partial embedding given by \mathcal{G} . The cycles (a), (b), and (d) from Fig. 9 are clearly hamiltonian. To check cycle (c), begin tracing the cycle starting with the edge x_0y_0 and then y_0x_2 . Observe that after x_2 the cycle begins a regular pattern, and traces (on the x side)

$$x_5, x_6, x_9, x_{10}, \dots, x_{4s+1}, x_{4s+2}, \dots$$

Since $n-3 \equiv 1 \pmod{4}$, the walk will contain the vertices x_{n-3} , x_{n-2} , x_1 , after which it will proceed to the x vertices whose subscripts are congruent to 3 and 4 (modulo 4). Thus we see that (c) is indeed a hamilton cycle.

To verify that each vertex has a valid local rotation it is enough to check that the local rotation about each vertex contains no 2-cycle and no 3-cycle. We must check the vertices x_0 , x_1 , x_2 , y_0 ,

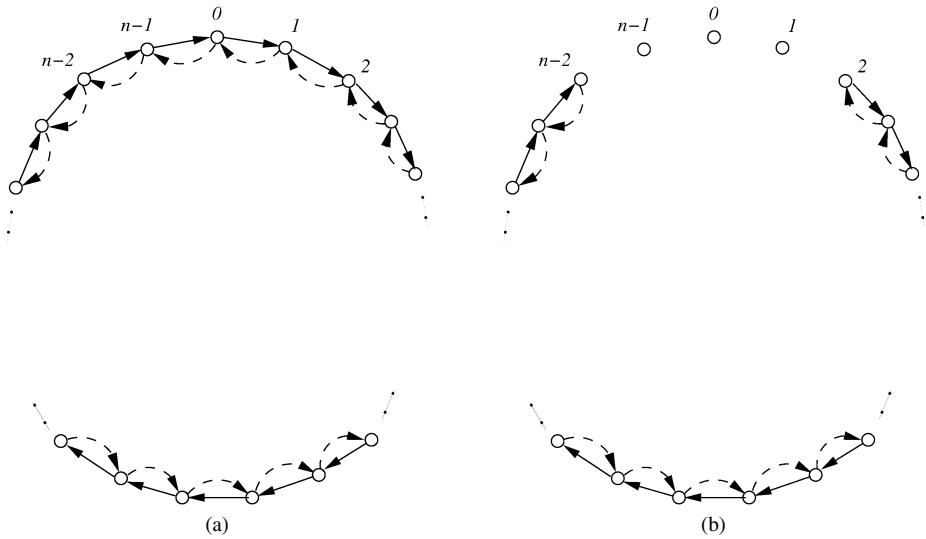


Fig. 8. A transition graph, and a partial one, for $K_{n,n}$.

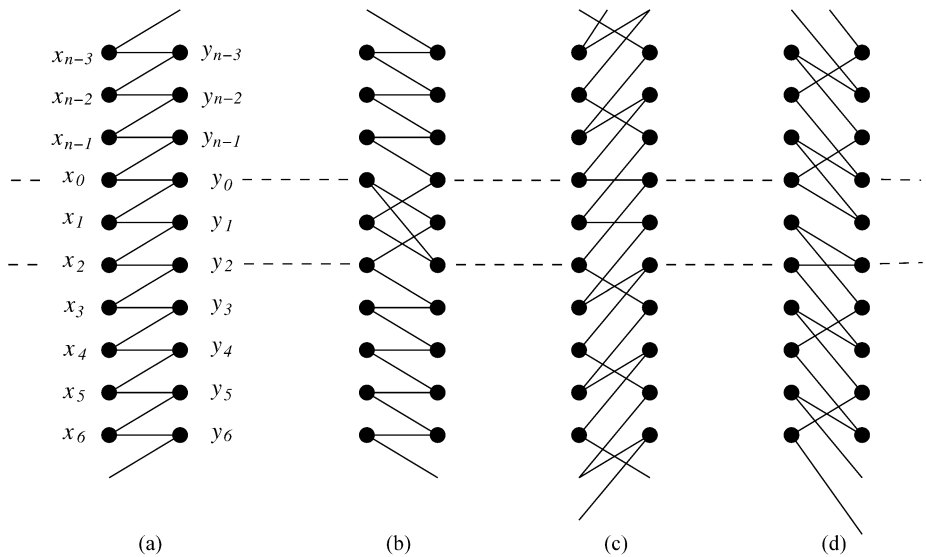


Fig. 9. Facial walks for $K_{n,n}$, $n \equiv 0 \pmod{4}$.

y_1 , and y_2 , and then (because of symmetry) we need only check two other vertices from each part of the bipartition, say x_3, x_4, y_3 and y_4 . If the local rotation at a vertex v contains a 3-cycle, the support of that 3-cycle must consist of the edges of slopes $n - 1, 0$, and 1 , which would imply that at v there is a transition $2 \sim (n - 2)$. Inspection shows that no such transition occurs. A 2-cycle in the local rotation at v means that at some vertex v there is a pair of consecutive edges $\{va, vb\}$ which appears in two of the faces given by Fig. 9. Again, inspection shows that such a situation does not occur.

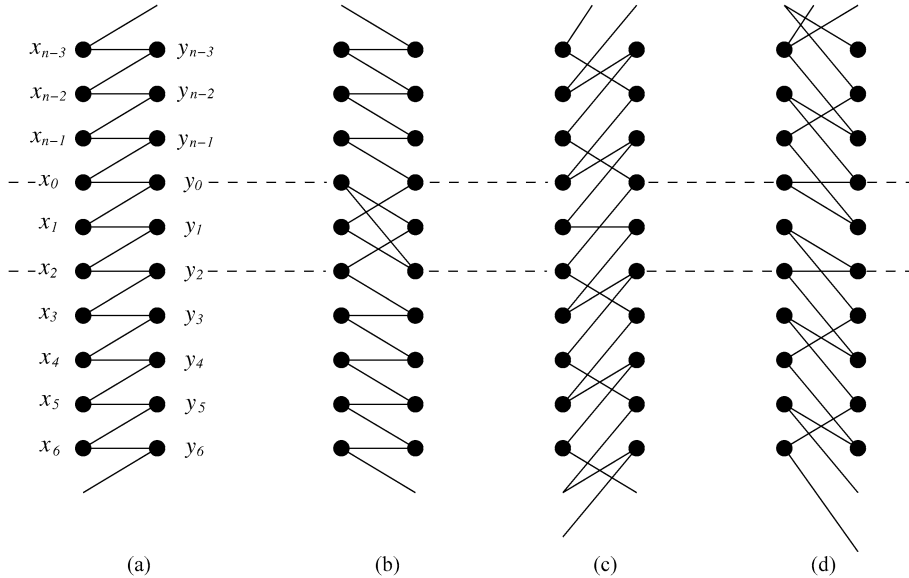


Fig. 10. Facial walks for $K_{n,n}$, $n \equiv 1 \pmod{4}$.

To verify nonorientability, observe that the cycles in Fig. 9(a) and (b) both contain the edges x_1y_0 and x_3y_3 , and in any orientation of the cycle in (a) these two edges must have opposite left-to-right orientations, while in any orientation of the cycle in (b) they must have the same left-to-right orientation. Therefore the cycles in (a) and (b) cannot be given a consistent orientation, and the embedding is consequently nonorientable. This completes the case where $n \geq 8$. For $n = 4$, one may omit the transition graph and use the four hamilton cycles given in Fig. 9.

Next suppose $n \equiv 1 \pmod{4}$, $n \geq 5$. Figure 10 shows the facial cycles we add to the partial embedding given by \mathcal{G} . Again, (a), (b), and (d) are clearly hamiltonian. One may verify the hamiltonicity of (c) just as in the case $n \equiv 0 \pmod{4}$. Verification of nonorientability is exactly the same as in the case $n \equiv 0 \pmod{4}$, since cycles (a) and (b) are essentially unchanged from that case. One verifies that local rotations are valid, and the case $n \equiv 1 \pmod{4}$ is completed for all $n \geq 5$.

The cycles for the case $n \equiv 3 \pmod{4}$ where $n \geq 7$ are given in Fig. 11. This case is similar to cases $n \equiv 0 \pmod{4}$ and $n \equiv 1 \pmod{4}$.

Finally, suppose $n \equiv 2 \pmod{4}$, $n \geq 6$. For this case, we use the cycles given in Fig. 12. Cycles (a) and (b) are clearly hamiltonian, and it is not difficult to verify that cycles (c) and (d) are as well. For nonorientability, the edges x_3y_3 and x_6y_5 must be have opposite left-to-right orientations in any orienting of (a), and the same left-to-right orientation in any orienting of (b). This completes the case $n \equiv 2 \pmod{4}$ where $n \geq 6$, and the proof of the claim. \square

4.2. Case II: m odd, n even

In this section we must show that (2) of Conjecture 1 holds for both $K_{m,m,n}$ and $K_{m+1,m,n}$.

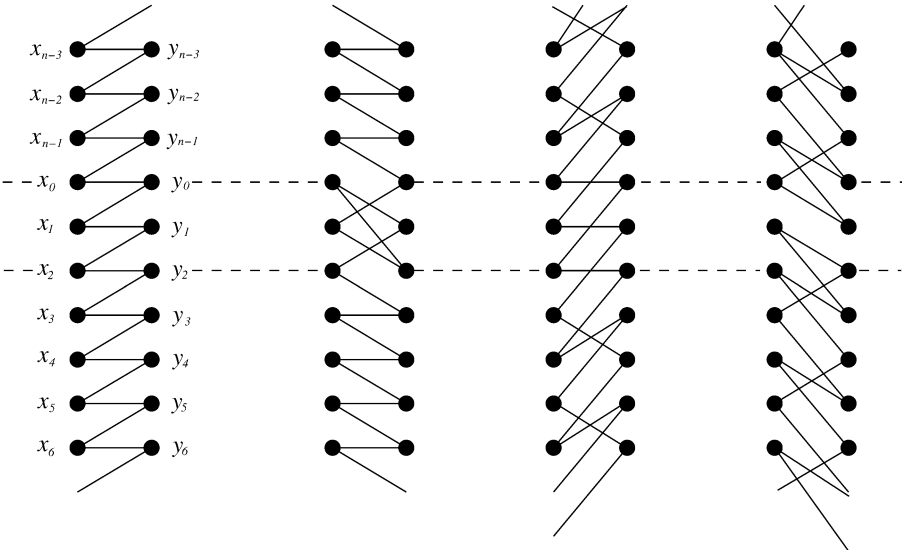


Fig. 11. Facial walks for $K_{n,n}$, $n \equiv 3 \pmod{4}$.

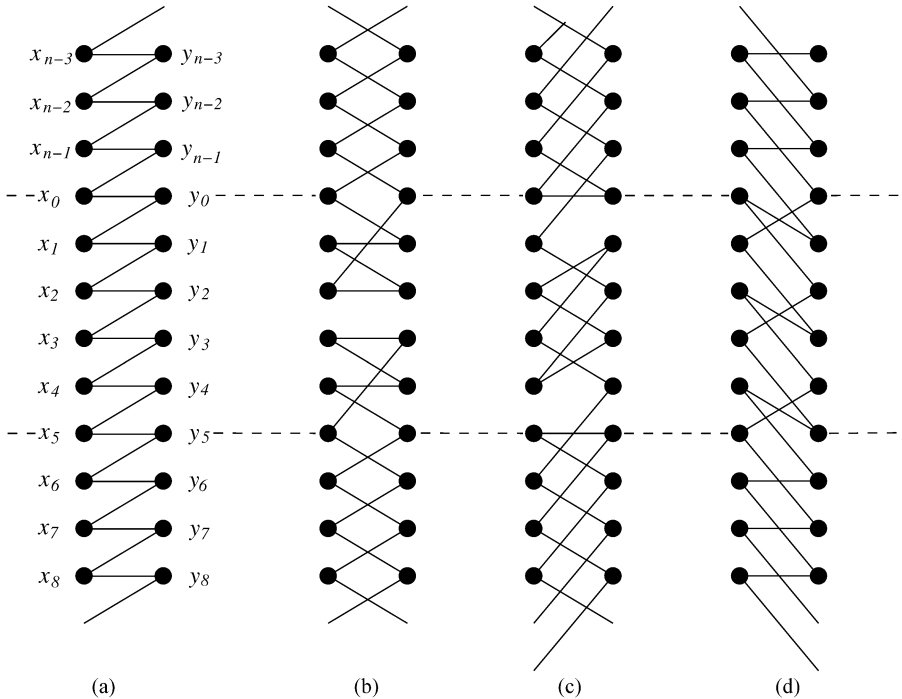


Fig. 12. Facial walks for $K_{n,n}$, $n \equiv 2 \pmod{4}$.

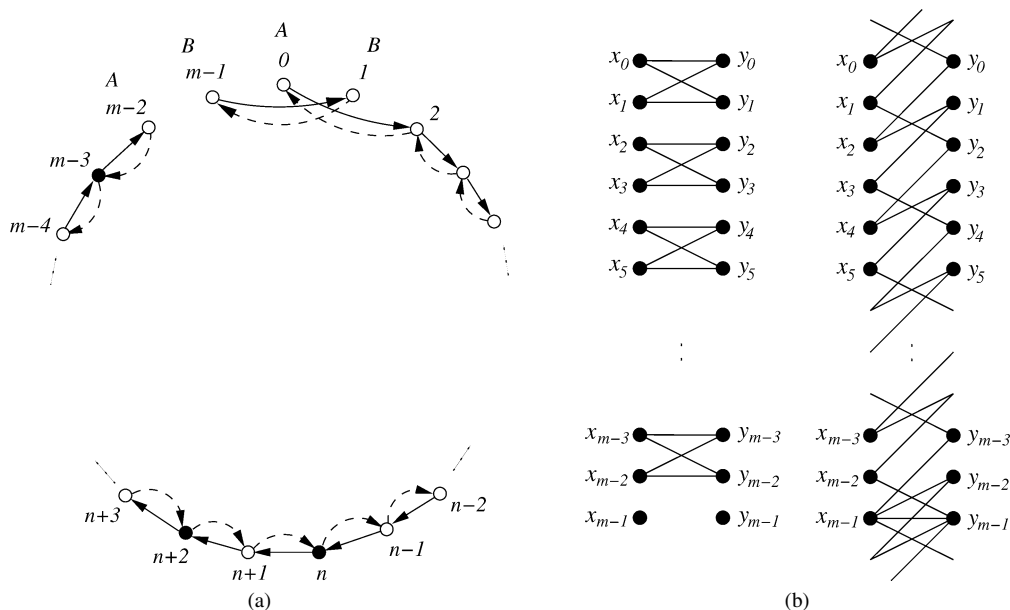


Fig. 13. A partial transition graph and some facial walks for m odd, $n \geq 4$ even.

Subcase $K_{m,m,n}$, where m is odd, $n \geq 4$, n even

Claim 13. Let m be odd and let $n \geq 4$ be even. Then there is an embedding of $K_{m,m,n}$ on the nonorientable surface of genus $\lceil (m-2)(m+n-2)/2 \rceil$.

Proof. A nonorientable embedding of $K_{5,5,4}$ on N_{11} may be found in [7]. Suppose $m \geq 7$ is odd and $n \geq 4$ is even. We begin with the partial transition graph shown in Fig. 13(a). We remark that for some vertices in the derived graph, orientations may be reversed on the component labeled B . This is because, in the terminology of Section 3.3, for each vertex v in the derived relative embedding corresponding to Fig. 13, the graph G_v has two components, namely, those corresponding to the components labeled A and B in Fig. 13. Thus, for such a v , the components of G_v are independent in terms of their orientations as parts of a local rotation at v , since either end of the component corresponding to A could still be connected to either end of the component corresponding to B .

Since $\gcd(2, m) = 1$, the boundary walk $F_0 = (0, 2, 0)$ corresponds to one facial hamilton cycle in the derived embedding. The boundary walks $F_i = (i, i+1, i)$, where $2 \leq i \leq n-2$, are hamilton cycles of type H. The boundary walks $D_i = (i, i+1, i, i-1, i)$, where $i = n, n+2, \dots, m-3$ are 4-cycles of type V. The edges linking $m-1$ and 1 represent the hamilton cycle consisting of all edges of slopes $m-1$ and 1 in the relative embedding; for reference, we label this boundary walk F_1 . Thus our partial transition graph yields $n-1$ facial hamilton cycles (corresponding to the F_i) and $(m-3-n)/2$ facial 4-cycles (corresponding to the D_i).

To this relative embedding we add faces with facial walks given in Fig. 13(b). Now Fig. 13(b) depicts $(m-1)/2$ 4-cycles on the left; on the right, we would like to have a facial walk of length $2m+2$ where we will put one of the vertices of the third part of the tripartition, but we must be careful about the way we define the transitions at x_{m-1} and y_{m-1} . Define the transitions at

x_{m-1} to be $(m-2) \rightarrow (m-1)$ and $1 \rightarrow 0$. If $m \equiv 1 \pmod{4}$ then define the transitions at y_{m-1} to be $0 \rightarrow (m-1)$ and $1 \rightarrow (m-2)$; if $m \equiv 3 \pmod{4}$ then define the transitions at y_{m-1} to be $0 \rightarrow 1$ and $(m-1) \rightarrow (m-2)$. We claim that these constraints give us a facial walk of length $2m+2$.

To verify that we do indeed get such a walk, suppose $m \equiv 1 \pmod{4}$. Begin tracing the walk with the edge $y_{m-1}x_1$ and then x_1y_2 . Following this path, we encounter (on the x side) vertices

$$x_1, x_4, x_5, x_8, x_9, \dots, x_{4s}, x_{4s+1}, \dots$$

until we come to x_{m-4} , then

$$y_{m-3}, x_{m-1}, y_{m-2}, x_0, y_{m-1}, x_{m-1}, y_0, x_3,$$

whence we proceed to x_2, x_3, \dots , which clearly gives us the single long walk we want. The case $m \equiv 3 \pmod{4}$ is similar.

Now we have $(m-3-n)/2 + (m-1)/2$ facial 4-cycles, $n-1$ facial hamilton cycles, and 1 facial walk of length $2m+2$. An application of Euler's formula shows that such faces yield an embedding on a surface with the conjectured genus, provided the local rotations are valid. A partial rotation at each vertex is given by the partial transition graph. This partial rotation consists of two transition paths, which we have labelled A and B in Fig. 13(a). A has endpoints 0 and $m-2$, and B has endpoints $m-1$ and 1. But we observe that in the supplementary faces we have given in Fig. 13(b), the additional transitions at any vertex are either $0 \leftrightarrow 1$ and $(m-2) \leftrightarrow (m-1)$ or $0 \leftrightarrow (m-1)$ and $(m-2) \leftrightarrow 1$. In any case, we are connecting endpoints of A with endpoints of B , giving us a cycle. Thus we have a valid embedding.

Finally, nonorientability is seen by applying Theorem 9 to the sequence of vertices $(n-2, n-1, n, n-1)$. \square

Subcase $K_{m,m,n}$ where m is odd and $n=2$

Claim 14. *Let m be odd and let $n=2$. Then there is an embedding of $K_{m,m,n}$ on the nonorientable surface of genus $\lceil (m-2)(m+n-2)/2 \rceil$.*

Proof. Appropriate minimal nonorientable embeddings for $K_{3,3,2}$ and $K_{5,5,2}$ are found in [7]. An appropriate minimal nonorientable embedding of $K_{7,7,2}$ can be found in Appendix A.

For $m \geq 9$, this case is similar to the previous one. Again we start with a partial transition graph and supplement with explicit facial walks. In fact, the supplementary facial walks are again the ones in Fig. 13(b). We must alter the partial transition graph, though, to one which yields only one hamilton cycle.

There are two partial transition graphs shown in Fig. 14. As in the discussion related to Fig. 13, for some vertices in the derived graph, orientations may be reversed on the components labeled A . Part (a) corresponds to the case $m \equiv 3 \pmod{4}$, $m \geq 11$, and part (b) corresponds to the case $m \equiv 1 \pmod{4}$, $m \geq 9$. In both cases, k is chosen so that $\gcd(k+1, m) = 1$ (m is odd, and $k+1$ is either $m-2$ or $m-4$) and $k \equiv 2 \pmod{4}$. Thus the boundary walk $(0, k+1, 0)$ corresponds to a single hamilton cycle in the derived embedding. Moreover $k/2$ is odd, so $k/2+1$ and k are both even, so that we may decompose the portion of the partial transition graph between $k/2+1$ and k into 4-cycles of type V, as shown in Fig. 14. Also $k/2-2$ is odd, so we may similarly decompose the portion of the partial transition graph between 1 and $k/2-2$ into 4-cycles of type V. $(m-1, k/2, k, k/2-1, m-1)$ is a 4-cycle of type X, as is $(k/2, k/2+1, k/2-1,$

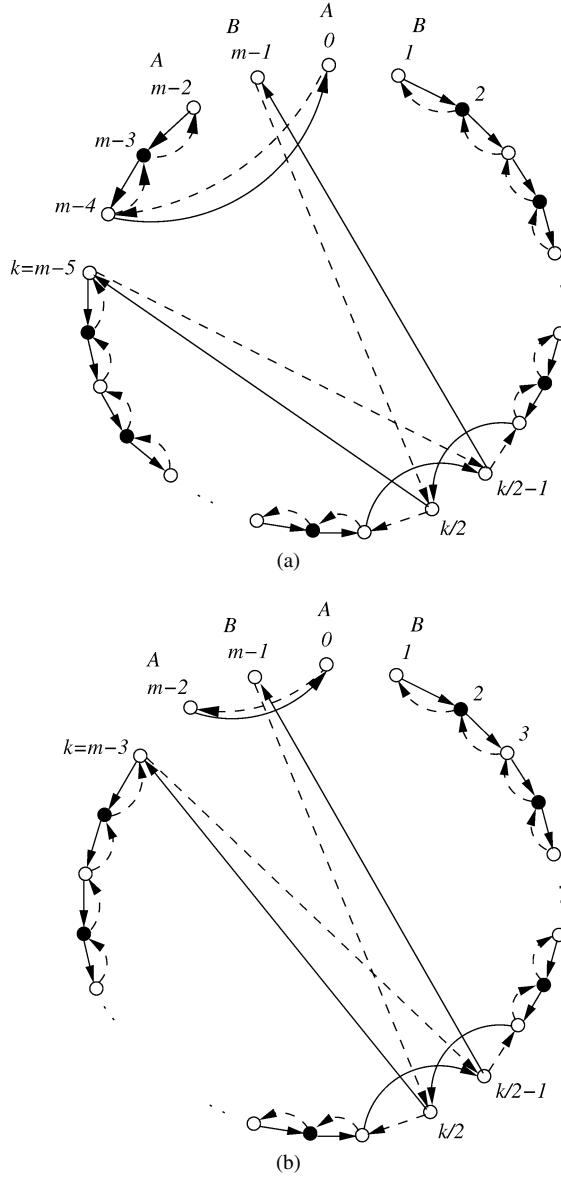


Fig. 14. Partial transition graphs for m odd, $n = 2$.

$k/2 - 2, k/2$). As in the previous case, the partial transition graph consists of two paths, labelled A and B , in both the solid and the dashed edges (the dashed paths are slightly different from the solid ones, but their endpoints are the same). The endpoints of these paths are as in the previous case, so the local rotations are all valid. Thus we have constructed an embedding of $K_{m,m}$ such that one face is a hamilton cycle, one face is of length $2m + 2$, and all other faces are 4-cycles. Applying Theorem 9 to the sequence of vertices $(k/2, k/2 + 1, k/2 + 2, k/2 + 1)$ gives nonorientability, and Euler's formula shows that the genus is as conjectured. \square

Completing Case II: $K_{m+1,m,n}$

Claim 15. Theorem 10 is true for the case m odd, n even.

Proof. The previous two claims verify the result for $l = m$, i.e., $K_{m,m,n}$. However, in the case of m odd, n even, Theorem 2 does not produce all the desired embeddings of all $K_{l,m,n}$ from those of $K_{m,m,n}$. In this case, we also need embeddings of $K_{m+1,m,n}$ in order to obtain embeddings for $K_{l,m,n}$ for all l . Thus, we need embeddings of the complete tripartite graphs $K_{2s+2,2s+1,2t}$ ($t \leq s$), and we have embeddings of the graphs $K_{2s+1,2s+1,2t}$ ($t \leq s$). The case $K_{4,3,2}$ is found in [7]. The cases $K_{6,5,2}$ and $K_{8,7,2}$ are found in Appendix A.

We handle the remaining cases by brute force; given the embedding of $K_{2s+1,2s+1,2t}$ constructed above, we add one vertex, add some crosscaps, and add edges. Specifically, the conjectured genus of $K_{2s+2,2s+1,2t}$ is

$$\left\lceil \frac{(2s+2-2)(2s+1+2t-2)}{2} \right\rceil = 2s^2 + 2st - s$$

and the known genus of $K_{2s+1,2s+1,2t}$ is

$$\left\lceil \frac{(2s+1-2)(2s+1+2t-2)}{2} \right\rceil = \left\lceil 2s^2 + 2st - 2s - t + \frac{1}{2} \right\rceil = 2s^2 + 2st - 2s - t + 1.$$

Thus we may add

$$(2s^2 + 2st - s) - (2s^2 + 2st - 2s - t + 1) = s + t - 1$$

crosscaps.

Consider the embedding of $K_{2s+1,2s+1}$ with $2t$ facial walks of length at least $2s+1$, where $t \geq 2$, given in Section 4.2. Let $m = 2s+1$, $n = 2t$. As in Fig. 13(b), let us call the vertices in the first part of the partition x_0, \dots, x_{m-1} , and the vertices in the second part of the partition y_0, \dots, y_{m-1} . Now of the $2t$ large faces, $2t-1$ of them are hamilton cycles and the other (the one on the right in Fig. 13(b)) has boundary of length $2m+2$. Call this long walk W . Add $2t-1$ vertices v_1, \dots, v_{2t-1} into the $2t-1$ hamilton cycle faces, add a vertex v_0 into W , and draw the appropriate edges so that we now have a minimal nonorientable embedding of $K_{2s+1,2s+1,2t}$. Now W has an edge $e = x_{m-1}y_{m-1}$. Since x_{m-1} and y_{m-1} appear twice each on W , when we add edges from v_0 to the vertices of W we may choose to draw edges $v_0 \sim x_{m-1}$ and $v_0 \sim y_{m-1}$ to the occurrences of x_{m-1} and y_{m-1} on W away from e . Thus, in our embedding of $K_{m,m,n}$ there is a facial 5-cycle F , either $v_0x_0y_{m-1}x_{m-1}y_0v_0$ or $v_0x_{m-2}y_{m-1}x_{m-1}y_0v_0$, depending on the value of $m \pmod{4}$. Once we add the v_i 's, the local rotation at x_{m-1} becomes $y_{m-1}v_{i_1}y_1v_{i_2}y_2v_{i_3}y_3 \dots y_{n-3}v_{i_{n-2}}y_{n-2}y_{n-1}y_n \dots y_{m-4}y_{m-3}v_0y_{m-2}v_{i_{n-1}}y_0y_{m-1}$. (See Fig. 15.)

We want to add one vertex x^* to the x -class, and connect it with all y - and v -vertices. We place x^* in the facial 5-cycle F , and connect it with all y - and v -vertices in that face. That leaves $m-2$ y -vertices and $n-1$ v -vertices to be reached, for a total of $2s+2t-2$ vertices. Since we may add $s+t-1$ crosscaps, it is enough that we reach two new vertices with each crosscap. We may do so by “skipping” every other face, as in Fig. 16. In this way we reach, successively, v_{i_1} and y_1 , then v_{i_2} and y_2 , and so on, until we get to $v_{i_{n-2}}$ and y_{n-2} , then y_{n-1} and y_n, \dots, y_{m-4} and y_{m-3} ; next we skip v_0 and reach y_{m-2} and $v_{i_{n-1}}$ with the final crosscap. So after adding these crosscaps, F becomes part of one large face with all y -vertices and all v -vertices on the boundary. Now we may connect x^* with all remaining y - and v -vertices and we have the desired embedding of $K_{2s+2,2s+1,2t}$, $t \geq 2$.

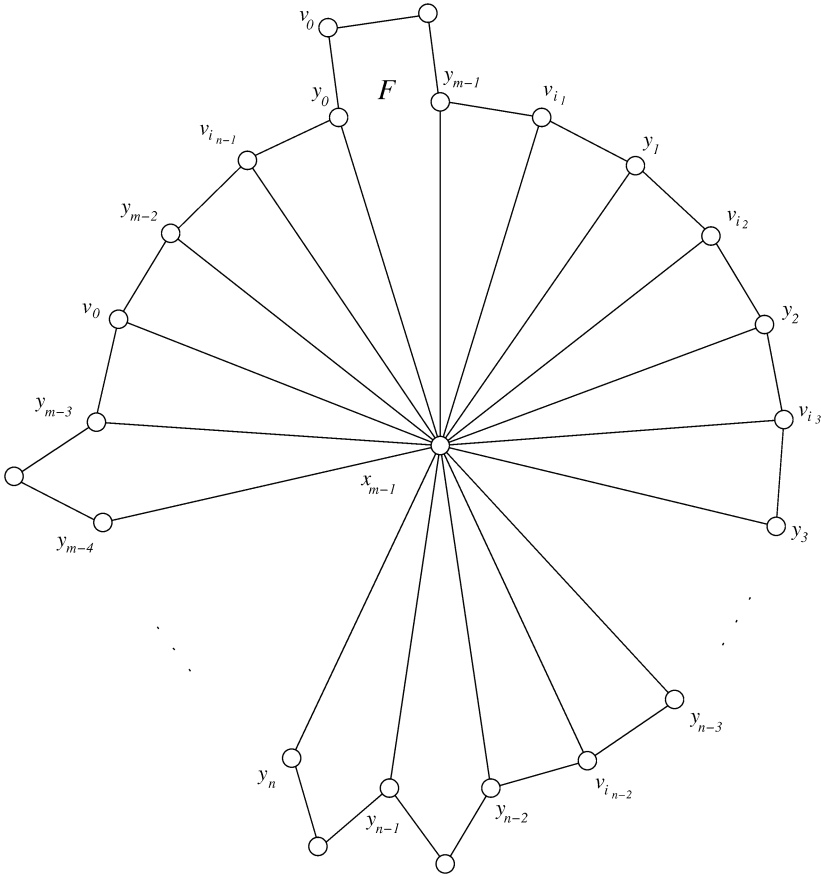


Fig. 15. Rotation at x_{m-1} .

Observe that in the above proof, the fact that enables us to reach two new vertices with each added crosscap is the following. If we step from face to face about x_{m-1} from the face F to the next occurrence of a face containing the vertex v_0 (in either direction), we will take an odd number of steps. This fact is guaranteed by the partial transition graph of Fig. 13, because the appearances of v_0 about x_{m-1} correspond to the “gaps” in the partial transition graph. But the gaps are an odd distance apart in the local rotation at x_{m-1} because the component labeled B in the figure corresponds to one hamilton face in the embedding of $K_{2s+1, 2s+1}$, which, after adding the third part of the tripartition, creates two triangular faces incident with x_{m-1} .

One may see that the same situation is present in either of the partial transition graphs of $K_{2s+1, 2s+1}$ with 2 facial hamilton cycles given in Fig. 14. That is, the components labeled A correspond to odd distances about x_{m-1} between consecutive faces containing v_0 , where v_0 is the vertex corresponding (as above) to the long cycle from Fig. 13(b). The component labeled A in Fig. 14(b) is similar to the component labeled B in Fig. 13(a), which we covered above. For Fig. 14(a), we observe that the edges $(m-4) \sim 0$ correspond to a hamilton facial cycle in the derived embedding, and so will contribute two triangular faces once we add the third part of the tripartition; the edges $(m-2) \sim (m-3)$ and similarly the edges $(m-3) \sim (m-4)$ correspond to facial 4-cycles in the derived embedding, and thus each contribute one face about x_{m-1} . Then

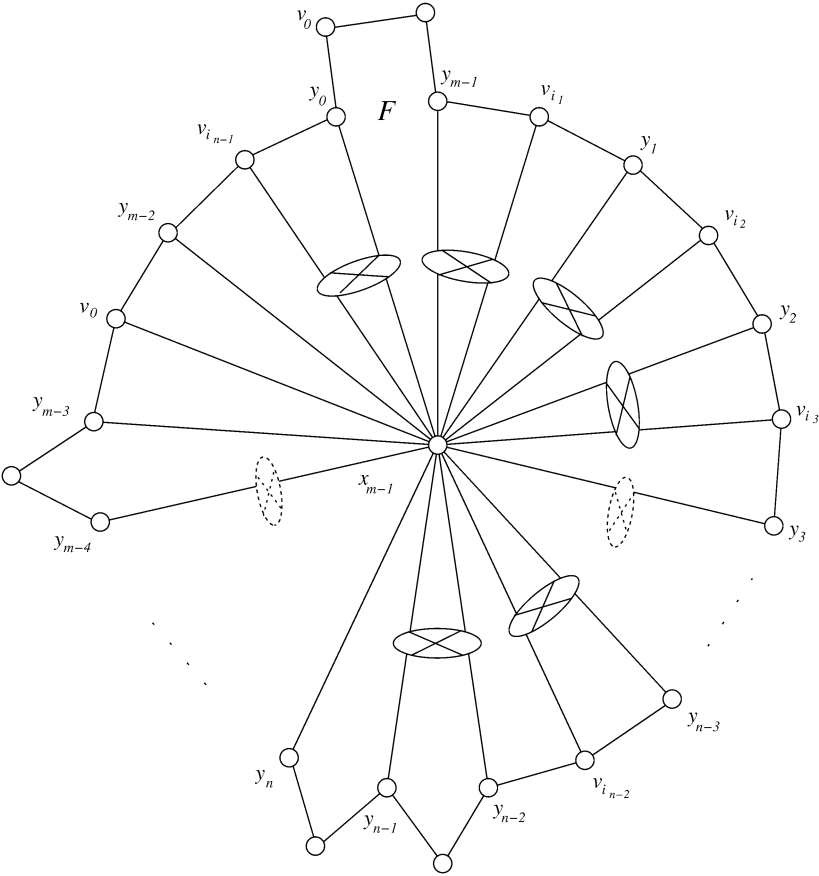


Fig. 16. Adding crosscaps around x_{m-1} .

there are exactly four faces about x_{m-1} that lie strictly between the faces containing x_{m-1} and v_0 , so that those faces are at an odd distance (about x_{m-1}) as claimed. Thus we may add crosscaps as in the case $t \geq 2$, and obtain the required embeddings of $K_{m+1,m,n}$, completing the proof of the claim. \square

4.3. Case III: m even, n odd

Subcase $m \equiv 2 \pmod{4}$, n odd

Claim 16. Theorem 10 is true in the case $m \equiv 2 \pmod{4}$, n odd.

Proof. We again prove the basis case $l = m$ by examining $K_{m,m,n}$, and the claim then follows for $l > m$ by Theorem 2. Any $K_{m,m,n}$ with $m \leq 2$ is planar. A minimal nonorientable embedding of $K_{6,6,1}$ is shown in Appendix A.

Suppose $m \equiv 2 \pmod{4}$, $m \geq 10$, and $n = 1$. Write $m = 2s$, where s is odd. The transition graph for this case is shown in Fig. 17, where k is some even number between 0 and s . Observe that the boundary walks $(0, s, 0)$, $(k, s + k, k)$, and $(k + 1, s + k + 1, k + 1)$ are 4-cycles of type I,

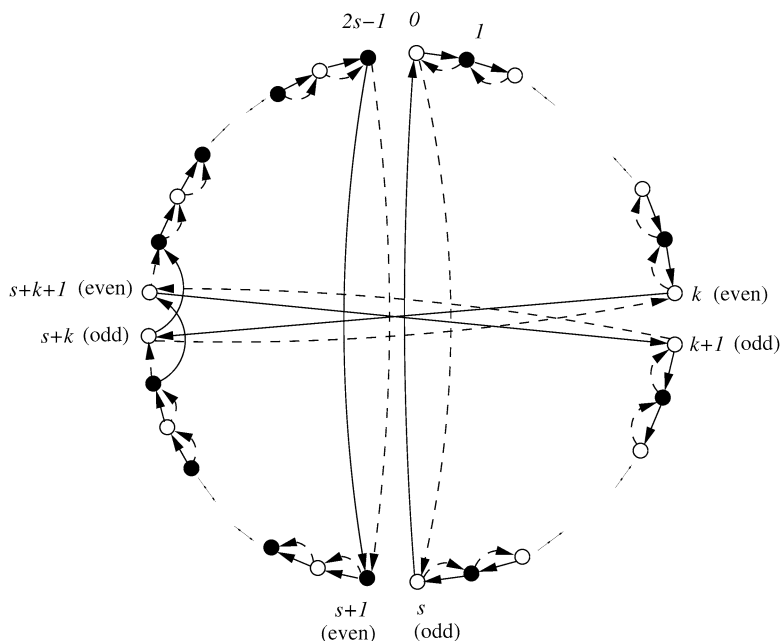


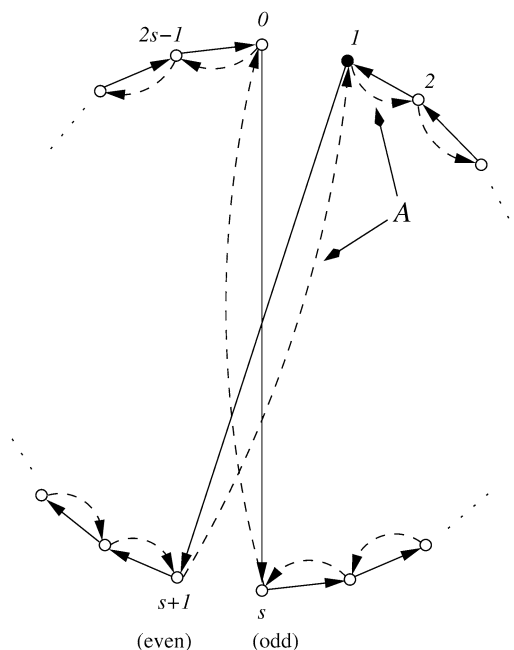
Fig. 17. Transition graph for $m \equiv 2 \pmod{4}$, $m \geq 6$, $n = 1$.

and the segments of the graph from 0 to k , $k+1$ to s , $s+1$ to $s+k-1$, and $s+k+2$ to $m-1 = 2s-1$ all have even length, and hence may be filled out with 4-cycles of type V (as in Fig. 17). The boundary walk $(s+k+1, s+k+2, s+k, s+k-1, s+k+1)$ is a 4-cycle of type X, and the boundary walk $(2s-1, s+1, 2s-1)$ corresponds to a hamilton cycle since $\gcd(s-2, 2s) = 1$. Applying Theorem 7 to the sequence of vertices $(s+k, s+k+1, s+k+2, s+k+1)$ gives nonorientability.

(The preceding proof may be adapted to any n , $1 < n \leq m-5$. We simply change the signature on the middle vertex of $(n-1)/2$ of the 4-cycles of type V (i.e., change the vertex from solid to open or vice versa). This transforms those $(n-1)/2$ 4-cycles of type V into $n-1$ hamilton cycles of type H. Euler's formula verifies the embedding is on the conjectured minimal nonorientable surface. However, we handle all cases $n \geq 3$ in another way below.)

Now suppose $m \equiv 2 \pmod{4}$, $m \geq 6$, and suppose that $n \geq 3$ is odd. Write $m = 2s$ where s is odd. The transition graph for the case $n = m-1$ is shown in Fig. 18. The boundary walk $(0, s, 0)$ is a 4-cycle of type I. The segments of the graph from 2 to s and from $s+1$ to 0 are filled in with hamilton cycles of type H. The boundary walk $A = (1, s+1, 1, 2, 1)$ has net voltage $s+1$ and length 4; $\gcd(s+1, 2s) = 2$, so A corresponds to 2 cycles of length $4 \cdot s$, that is, two hamilton cycles. Thus the transition graph in Fig. 18 gives a total of n hamilton cycles and $m/2$ 4-cycles. Euler's formula verifies that this embedding has the conjectured genus. For $3 \leq n < m-1$, replace the type-H hamilton cycles two at a time by type-V 4-cycles, starting with $(3, 4, 3)$ and $(5, 4, 5)$ (as above, this is effected by changing the signature on the vertex the two type-H cycles have in common—for example, we start by changing vertex 4 from open to solid). Applying Theorem 7 to the sequence of vertices $(1, 2, 3, 2)$ gives nonorientability.

This completes the proof of the claim. \square

Fig. 18. Transition graph for $m \equiv 2(4)$, $m \geq 6$, $n = m - 1$.

Subcase $m \equiv 0 \pmod{4}$, n odd, $n \geq 3$

Claim 17. Theorem 10 is true in the case $m \equiv 0 \pmod{4}$, n odd, $n \geq 3$.

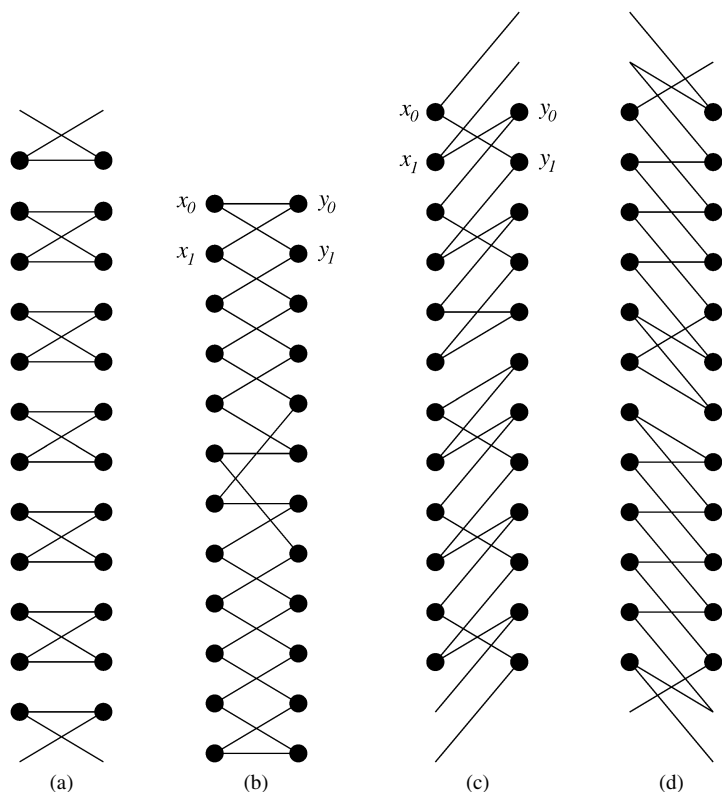
Proof. As usual, we prove the basis case $l = m$ by examining $K_{m,m,n}$, and the claim then follows for $l > m$ by Theorem 2. Recall that $K_{4,4,3}$ does not conform to Eq. (2). It is handled in [7]. Thus we need to use $K_{5,4,3}$ and $K_{6,4,3}$ as bases for the induction in place of $K_{4,4,3}$. An embedding for $K_{5,4,3}$ satisfying Eq. (2) is provided in [7]; one for $K_{6,4,3}$ is provided in Appendix A.

Suppose $m \equiv 0 \pmod{4}$, $m \geq 8$, $n \geq 3$. For the case $n = m - 1$, we begin with the partial transition graph found in Fig. 8. For $3 \leq n < m - 1$, we replace the type-H hamilton cycles two at a time with 4-cycles of type V. Then we supplement the resulting partial transition graph with $m/2$ 4-cycles and 3 hamilton cycles as shown in Fig. 19 for the case $m = 12$. One may check that all local rotations are valid. For nonorientability, observe that the edges x_0y_1 and x_1y_0 must have the same left-to-right orientation in any orienting of the cycle in Fig. 19(b), and opposite orientations in any orienting of the cycle in Fig. 19(c). Euler's formula shows that the genus of this embedding is as in Eq. (2). This completes the proof of the claim. \square

Subcase $m \equiv 0 \pmod{4}$, $n = 1$

Claim 18. Theorem 10 is true in the case $m \equiv 0 \pmod{4}$ and $n = 1$.

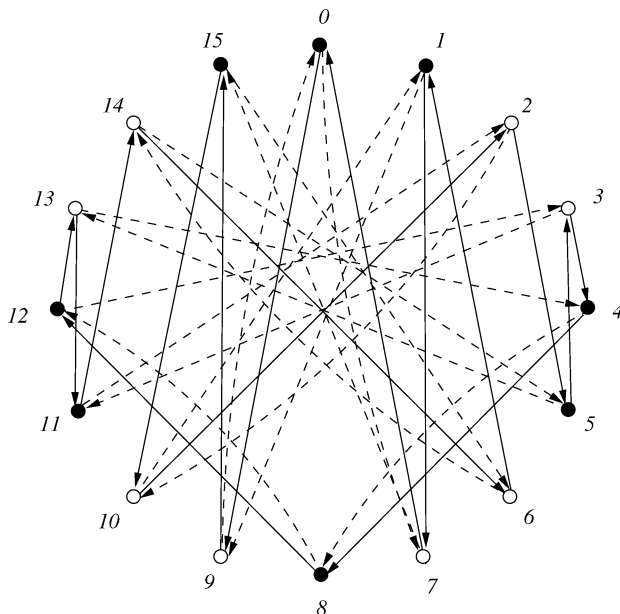
Proof. We prove the basis case $l = m$ by examining $K_{m,m,1}$, and the claim then follows for $l > m$ by Theorem 2. Recall that $K_{4,4,1}$ does not conform to Eq. (2). It is handled in [7]. Thus, we must

Fig. 19. Facial walks for $K_{12,12,n}$, n odd, $n \geq 3$.

use $K_{5,4,1}$ and $K_{6,4,1}$ as bases for the induction. An embedding for $K_{5,4,1}$ satisfying Eq. (2) is provided in [7]; one for $K_{6,4,1}$ is provided in Appendix A.

Suppose $m \equiv 0 \pmod{4}$, $m \geq 8$, and $n = 1$. For this case we must use a more complicated construction. To outline the proof, we first find a minimal embedding of the bipartite graph $K_{m,m}$ with the property that the vertices in one part of the partition all “see” each other. Next, we perform a diamond sum of this embedding with a minimal embedding of $K_{m,3}$ to get a minimal genus embedding of $K_{m+1,m}$. Finally, we connect one of the “ $m+1$ ” vertices with all the others, giving us $K_{m,m,1}$.

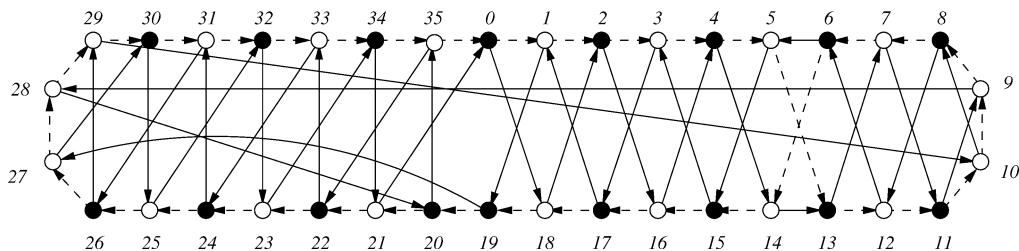
Let us say $K_{m,m}$ has bipartition (U, V) where $U = \{u_0, \dots, u_{m-1}\}$ and $V = \{v_0, \dots, v_{m-1}\}$. We want to find a minimal embedding Π of this graph so that for any pair of vertices u_i, u_j in U , there is some face of Π containing both u_i and u_j . This is not so hard using transition graphs. For instance, let \mathcal{G} be a cyclic m -transition graph with solid edges representing the rotations of the V side, and dashed edges representing the rotations of the U side. Suppose also that there is a solid edge $j \sim (j+k)$ in \mathcal{G} which is part of the boundary walk A . Such a solid edge implies that for each $i = 0, \dots, m-1$ the vertex v_{i-j} is adjacent to u_i and u_{i+k} in some face corresponding to A . Thus, vertex u_i is in a face with the vertex u_{i+k} if there is a solid edge in the transition graph of “length” k , i.e., one of the form $j \sim (j+k)$ for some j . Thus, for the embedding we want, it suffices to find a cyclic m -transition graph \mathcal{G} such that for every k , $1 \leq k \leq m/2$, there is an edge $j \sim (j+k)$ for some j , and such that every face in the derived graph is a 4-cycle.

Fig. 20. Transition graph for $K_{16,16,1}$.

In addition (for reasons that will become clear), we would like there to be two solid edges of length $m/2$ that are an odd distance apart in the solid hamilton cycle.

We handle the problem in two cases, namely $m \equiv 0 \pmod{8}$ and $m \equiv 4 \pmod{8}$. First, let $m = 8s$, $s \geq 1$. The transition graph for $m = 16$ is shown in Fig. 20. In general the transition graph is constructed as follows. We begin with a 4-cycle of type V having boundary walk $(0, 4s+1, 0, 4s-1, 0)$. Clearly this walk will yield solid edges of length $4s-1$. Next we construct a 4-cycle of type X with boundary walk $(4s-1, 1, 4s+1, 8s-1, 4s-1)$, in which the $1 \sim (4s-1)$ and $(4s+1) \sim (8s-1)$ edges are solid. This walk handles the solid edges of length $4s-2$. We continue in this fashion as in Fig. 20, until the 4-cycle of type X with boundary walk $(s-1, 3s, 7s+1, 5s, s-1)$ (with solid edges $(s-1) \sim 3s$ and $5s \sim (7s+1)$ of length $2s+1$) has been drawn. Next we construct 4-cycles of type I with boundary walks $(s, 5s, s)$ and $(3s, 7s, 3s)$, whose solid edges have length $4s = m/2$. Then we resume the construction of the progressively smaller 4-cycles of type X, finishing with the one with boundary walk $(2s-1, 2s, 6s+1, 6s, 2s-1)$ in which $(2s-1) \sim 2s$ and $(6s+1) \sim 6s$ are solid. Now for each k , $1 \leq k \leq 2s-1$ and $2s+1 \leq k \leq 4s-1$, we have a solid edge $j \sim (j+k)$ for some j . For the solid edges of length $2s$, we construct a 4-cycle of type V with boundary walk $(4s, 6s, 4s, 2s, 4s)$. A quick inspection verifies that the solid edges and the dashed edges each form a hamilton cycle. It remains to orient each cycle, and assign vertex signatures; ones analogous to those in Fig. 20 will do. Finally, the solid edges of the two 4-cycles of type I are at a distance of $4s-1$ in the solid hamilton cycle (where by the distance between two edges we mean the distance of their corresponding vertices in the line graph).

Suppose $m = 8s+4$, $s \geq 2$. The transition graph for $m = 36$ is shown in Fig. 21. In general we construct the desired cyclic m -transition graph in the following way. We begin with a 4-cycle of type X, with boundary walk $(0, 4s+2, 4s+3, 1, 0)$, in which the $0 \sim (4s+2)$ and $1 \sim (4s+3)$ edges of length $4s+2$ are solid. This handles the edges of length $m/2 = 4s+2$. Next we construct

Fig. 21. Transition graph for $K_{36,36,1}$.

a 4-cycle of type X with boundary walk $(0, 4s+5, 4s+4, 8s+3, 0)$ in which the $0 \sim (4s+5)$ and $(8s+3) \sim (4s+4)$ edges of length $4s-1$ are solid. This handles the solid edges of length $4s-1$. Next we construct a 4-cycle of type X with boundary walk $(8s+3, 4s+6, 4s+5, 8s+2, 8s+3)$ in which the $0 \sim (4s+5)$ and $(8s+3) \sim (4s+4)$ edges are solid. This handles the solid edges of length $4s-3$. We continue in this manner, constructing 4-cycles of type X whose solid edges have odd length, until we have drawn the edges of length 3. Then we do the same thing with the even edges, beginning with $(1, 4s+1, 4s+2, 2, 1)$, with solid edges $1 \sim (4s+1)$ and $2 \sim (4s+2)$, of (even) length $4s$. We make one exception, though, when constructing the even edges. Namely, when we construct the 4-cycle of type X $(s+1, 3s+1, 3s+2, s+2, s+1)$, we draw the edges of length 1 (i.e., $(s+2) \sim (s+1)$ and $(3s+2) \sim (3s+1)$) solid, and the edges of length $2s$ (i.e., $(s+1) \sim (3s+1)$ and $(s+2) \sim (3s+2)$) dashed. At this point we have drawn solid edges of length k for each odd k , $1 \leq k \leq 4s-1$, and each even k , $2 \leq k \leq 4s+2$ except for $k=2s$. We then draw a 4-cycle of type X with boundary walk $(4s+3, 6s+3, 6s+4, 4s+4, 4s+3)$, in which the edges $(4s+3) \sim (6s+3)$ and $(4s+4) \sim (6s+4)$ of length $2s$ are solid. This handles the solid edges of length $2s$. Finally, we draw a 4-cycle of type X with boundary walk $(2s+1, 6s+4, 6s+5, 2s+2, 2s+1)$, in which the edges of length $4s+1$ are solid.

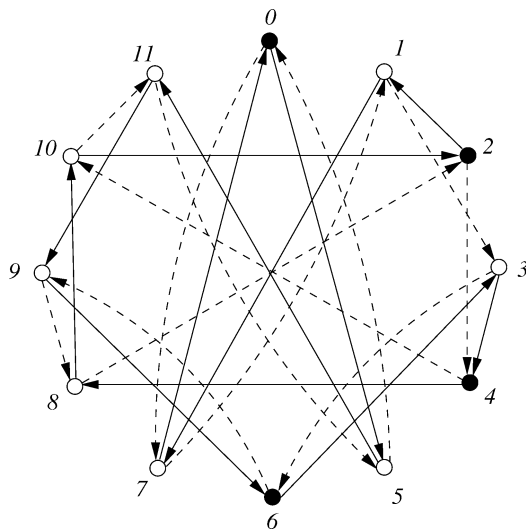
It is easy to see that the dashed edges yield a hamilton cycle: almost all dashed edges are of the form $j \sim (j+1)$. The solid edges are a bit more difficult, but the reader is encouraged to verify that they indeed form a hamilton cycle. It remains to fix an orientation on the cycles and to assign a signature to the vertices. One may choose an orientation and a signature in an analogous way to that shown in Fig. 21. Finally, the two solid edges of length $4s+2$ are at a distance of $2s+1$ in the solid hamilton cycle.

This construction fails for $m=12$. A special transition graph for $m=12$ is shown in Fig. 22. The graph has the required properties: all faces of the derived embedding are 4-cycles, all edge lengths occur, two solid edges of length $m/2$ appear at an odd distance apart (namely, 3).

Now we have the desired embedding Π of $K_{m,m}$ such that all faces are 4-cycles, and such that

- (1) for any pair of vertices u_i, u_j in U , there is some face of Π containing both u_i and u_j , and
- (2) there are two faces containing the vertices u_i and $u_{i+m/2}$, which are an odd distance apart in the local rotation at $u_{i+m/2}$.

In particular u_0 and $u_{m/2}$ share two faces. Now let Π' be a minimal genus embedding of $K_{m,3}$. Suppose the three vertices in the second part of the partition of $K_{m,3}$ are x, y , and z . Let $G = K_{m,m}$ and $G' = K_{m,3}$, and perform the diamond sum $\Pi(G, u_{m/2}) \diamond \Pi'(G', z)$. The resulting embedding is a minimal genus embedding of $K_{m+1,m}$, where the part with $m+1$ vertices consists of $U \setminus \{u_{m/2}\} \cup \{x, y\}$. We claim that we may add edges u_0x, u_0y , and u_0u_i for all i , $1 \leq i <$

Fig. 22. Transition graph for $K_{12,12,1}$.

$m/2$ and all i , $m/2 < i \leq m-1$. Certainly we may add all u_0u_i edges by condition (1) above. Now consider the embedding Π with respect to the vertex $u_{m/2}$. There exist two facial 4-cycles I_1 and I_2 containing both u_0 and $u_{m/2}$. Without loss of generality say $I_1 = u_0v_{j_1}u_{m/2}v_{j_2}$ and $I_2 = u_0v_{j_3}u_{m/2}v_{j_4}$. Moreover, since we identify the neighbors of z with the neighbors of $u_{m/2}$, there exist facial walks $J_1 = zv_{j_1}p_1v_{j_2}$ and $J_2 = zv_{j_3}p_2v_{j_4}$ in Π' , where p_i is either x or y for $i = 1, 2$. Then in $\Pi \diamond \Pi'$, we have new facial walks $u_0v_{j_1}p_1v_{j_2}$ and $u_0v_{j_3}p_2v_{j_4}$. Now in Π' , the v_j 's have only the neighbors x , y , and z . Moreover, all the faces in Π' are 4-cycles. Thus, if we follow the faces around z in, say, the clockwise direction, z sees alternately x, y, x, \dots . But by condition (2) above the facial cycles I_1 and I_2 in Π were an odd distance apart in the local rotation at $u_{m/2}$, and it follows that $p_1 \neq p_2$. Thus we may add the edges u_0x and u_0y , as claimed. Nonorientability is easy to see from the transition graph \mathcal{G} . (Alternatively, we may just insist that the embedding of $K_{m,3}$ is nonorientable.)

This completes the proof of the claim. \square

And that completes the proof of Theorem 10. \square

5. For further study

The most obvious direction for further research is to complete the corresponding orientable conjecture for the complete tripartite graphs. We have made some progress on this problem. In particular, we have verified Eq. (1) for $K_{l,m,n}$, $l \geq m \geq n$, when m is even, or n is odd, or both.

Another direction for further research is to consider complete p -partite graphs for $p > 3$. The conjectured value of the genus of $K_{l,m,n}$ can be regarded as coming from lower bounds obtained from the genus of complete bipartite subgraphs. The strongest such lower bound comes from $K_{l,m+n}$, and Conjecture 1 proposes that this bound is tight. For $K_{p,q,r,s}$, one may also obtain lower bounds on the genus by looking at the genus of complete bipartite subgraphs. If $p \geq q \geq r \geq s$, the strongest lower bound comes from either $K_{p,q+r+s}$ or from $K_{p+s,q+r}$, and so one obtains the following lower bounds on the genus of $G = K_{p,q,r,s}$:

- (1) If $p \geq q + r$ then $g(G) \geq \lceil \frac{(p-2)(q+r+s-2)}{4} \rceil$ and $\tilde{g}(G) \geq \lceil \frac{(p-2)(q+r+s-2)}{2} \rceil$.
 (2) If $p \leq q + r$ then $g(G) \geq \lceil \frac{(p+s-2)(q+r-2)}{4} \rceil$ and $\tilde{g}(G) \geq \lceil \frac{(p+s-2)(q+r-2)}{2} \rceil$.

In [12] Jungerman proved that the genus of $K_{n,n,n,n}$ is $(n-1)^2$ for $n \neq 3$, and in [13] Jungerman proved that the nonorientable genus of $K_{n,n,n,n}$ is $2(n-1)^2$ for $n \geq 3$. Both results realize the lower bound supplied in (2) above. On the other hand, it is also shown in [13] that $K_{2,2,2,2}$ has no embedding on the Klein bottle, so that for this graph (2) above is not tight. Bouchet has obtained several results about embeddings of complete equipartite graphs. Among these results is a new proof of the fact that $g(K_{n,n,n,n})$ is $(n-1)^2$ when n is not a multiple of 2, 3 or 5 [3].

Finally, define the *join* of two graphs G and H , written $G + H$, to be the graph with vertex set $V(G) \cup V(H)$ and edge set $E(G) \cup E(H) \cup \{xy \mid x \in V(G), y \in V(H)\}$. In the proof of Claim 18 we constructed minimal nonorientable embeddings of complete bipartite graphs $K_{4s,4s}$ with the property that for any two vertices u_i and u_j in a predetermined side U of the partition, there is a face F_{ij} containing both u_i and u_j . Clearly this can be extended to an embedding of $\overline{K_{4s}} + K_{4s}$ (taking U as the second side of the partition) by simply putting the edge $u_i u_j$ in the face F_{ij} for all $i \neq j$. We have obtained similar constructions for $K_{2s,2s}$, when s is odd, so that for any even m , it is true that

$$\tilde{g}(\overline{K_m} + K_m) = \tilde{g}(K_{m,m}).$$

Since $K_{l,m}$ is a subgraph of $\overline{K_l} + K_m$, it is always true that

$$g(\overline{K_l} + K_m) \geq g(K_{l,m}) \quad \text{and} \quad \tilde{g}(\overline{K_l} + K_m) \geq \tilde{g}(K_{l,m}).$$

Based on face size considerations and Euler's formula, we make the following conjecture.

Conjecture 19. *Let $m \geq 2$. Then, with finitely many exceptions,*

$$g(\overline{K_l} + K_m) = \begin{cases} \lceil \frac{(l-2)(m-2)}{4} \rceil = g(K_{l,m}), & \text{if } m \leq l+1, \\ \lceil \frac{(m-3)(m+2l-4)}{12} \rceil, & \text{if } m \geq l+1, \end{cases} \quad (3)$$

$$\tilde{g}(\overline{K_l} + K_m) = \begin{cases} \lceil \frac{(l-2)(m-2)}{2} \rceil = \tilde{g}(K_{l,m}), & \text{if } m \leq l+1, \\ \lceil \frac{(m-3)(m+2l-4)}{6} \rceil, & \text{if } m \geq l+1. \end{cases} \quad (4)$$

The need for exceptions is shown, for example, by $\tilde{g}(\overline{K_4} + K_5)$, which cannot satisfy the conjecture because $\overline{K_4} + K_5$ contains $K_{4,4,1}$, which does not satisfy the nonorientable part of Conjecture 1. Two of us (Ellingham and Stephens) have verified (4) above for $m \leq l+1$ and $(l, m) \neq (4, 5)$ —see [6] for this result, and for a discussion of previous results relevant to this conjecture.

Appendix A. Small cases

In this section we give those embeddings not obtained by the general construction. The embeddings appearing in this appendix were found by a computer search, and the format in which they appear here is the format in which the program outputs them. A description of the format is followed by the embeddings themselves.

A.1. Description of the embeddings

Let us suppose $K_{l,m,n}$ has tripartition $(X = \{x_1, x_2, \dots, x_l\}, Y = \{y_1, y_2, \dots, y_m\}, Z = \{z_1, z_2, \dots, z_n\})$. Then it may be regarded as the union of a complete bipartite spanning subgraph $H \cong K_{l,m+n}$ with bipartition $(X, Y \cup Z)$ and a complete bipartite subgraph $J \cong K_{m,n}$ with bipartition (Y, Z) . From this point of view, the complete tripartite genus conjectures are just strengthenings of Ringel's results on complete bipartite graphs. The conjectures say that if $l \geq m \geq n$ then $g(K_{l,m,n}) = g(K_{l,m+n})$ and $\tilde{g}(K_{l,m,n}) = \tilde{g}(K_{l,m+n})$. In other words, we can find an embedding of $H \cong K_{l,m+n}$ with the genus specified by Ringel's formula, in such a way that the edges of the $J \cong K_{m,n}$ can be added in the same surface, as chords of the faces. (Unfortunately, the embeddings of complete bipartite graphs given by Ringel do not seem to allow us to do this.)

So, we specify our embeddings of $K_{l,m+n}$ below by describing an embedding of $H \cong K_{l,m+n}$, along with the faces in which the edges of J , having the form $y_i z_j$, are to be inserted. The upper part of each description is an $l \times (m+n)$ table describing the embedding of H . The rows represent the vertices of X and the columns represent the vertices of $Y \cup Z$, with a vertical line dividing Y from Z . Each cell represents an edge of H , and contains two letters denoting the two faces to which the edge belongs (faces start at 'a'). Since the embeddings below do not require facial walks with repeated vertices, we can determine each facial cycle from the table. The lower left part of each description is an $n \times m$ table describing the embedding of J . The rows represent the vertices of Z and the columns represent the vertices of Y . Each cell contains one letter denoting the face of H into which the edge $y_i z_j$ is to be inserted. Since the embeddings below contain only 4- and 6-cycles as faces, and we insert edges incident with at most half of the vertices of a given face, we do not need to worry about edges crossing when more than one is inserted in a given face, which happens in some cases. The lower right part of each description lists a sequence of faces (not guaranteed to be minimal) that can be used to prove nonorientability.

To illustrate, in Fig. 23 we see the description of an embedding of $K_{4,3,2}$ on N_3 , with labels added. The face 'b' of H , for example, has facial walk $(x_1 z_1 x_3 y_1)$ from the upper part, and from the lower part we see that the edge $y_1 z_1$ of J is to be inserted in this face. Rotations around each vertex in H can be generated from the upper part of the description: for example, around vertex x_1 we can see that the faces occur in cyclic order (abdec) so the vertices appear in order $(y_1 z_1 y_3 z_2 y_2)$. The sequence 'gdbifa' shows that the embedding is nonorientable, as follows. Assume an orientation of faces exists, so that each edge is oriented once in each direction. Call the direction from X to $Y \cup Z$ down, and the opposite direction up. The edges of each face must be oriented alternately up and down. Without loss of generality we may orient $x_2 z_1$ up in 'g', so it must be down in 'd'. Then $x_1 z_1$ must be up in 'd' and down in 'b', $x_3 y_1$ must be down in 'b' and up in 'i', $x_4 y_1$ must be down in 'i' and up in 'f', and $x_2 y_1$ must be down in 'f' and up in 'a'. But now $x_2 y_2$ is down in both 'a' and 'g', a contradiction.

	y_1	y_2	y_3	z_1	z_2
x_1	ab	ac	de	bd	ce
x_2	af	ag	dh	dg	fh
x_3	bi	ci	hj	bj	ch
x_4	fi	gi	ej	gj	ef
z_1	b	g	j	gdbifa	
z_2	f	c	h		

Fig. 23. Illustration of embedding format.

A.2. Embeddings not covered by the general constructions

$K_{6,4,1}$ on N_6

ab	ac	bd	ce	de
af	ag	df	gh	dh
bi	cj	bk	ck	ij
fl	gm	fm	eg	el
in	mo	mn	ho	hi
ln	jo	kn	ko	jl
l	j	d	h	hdbi

$K_{6,4,3}$ on N_{10}

ab	ac	bd	ce	df	eg	fg
ah	ai	dh	ej	dk	ek	ij
bl	cm	bn	co	fo	lm	fn
hp	iq	hr	oq	op	gr	gi
ps	mt	ru	ju	pt	mr	js
ls	qt	nu	qu	kt	kl	ns
p	t	d	o	qujecmt		
l	m	r	e			
s	i	n	j			

$K_{6,5,2}$ on N_{10}

ab	ac	bd	ce	df	eg	fg
ah	ai	dh	ej	dk	ek	ij
bl	cm	bn	co	fo	lm	fn
hp	iq	hr	op	oq	gr	gi
ls	qt	rt	ju	qu	lr	js
ps	mt	nt	pu	ku	km	ns
l	m	r	e	k	oqukdblsph	
s	i	n	j	f		

$K_{6,6,1}$ on N_{10}

ab	ac	bd	ce	df	eg	fg
ah	ai	dh	ej	dk	ek	ij
bl	cl	bm	cn	fo	no	fm
hp	ip	hq	nr	qr	gn	gi
ls	lt	qu	ju	kq	kt	js
ps	pt	mu	ru	or	ot	ms
s	i	m	j	f	g	qkdblsph

$K_{7,7,2}$ on N_{18}

ab	ac	bd	ce	df	eg	fh	gi	hi
aj	ak	dj	ek	dl	em	hn	ln	hm
bi	co	bo	cp	fq	gr	fr	gp	iq
is	ks	tu	kt	lv	mw	vw	il	mu
jx	yz	jt	tA	vB	xB	nv	ny	zA
xC	oz	oD	pE	qC	rx	rE	pD	qz
sC	sy	uD	AE	BC	wB	wE	yD	uA
i	y	D	p	l	g	n	BvldbisCx	
i	z	u	A	q	m	h		

$K_{8,7,2}$ on N_{21}

ab	ac	bd	ce	df	eg	fh	gi	hi
aj	ak	dj	ek	dl	em	hn	ln	hm
bo	co	bp	cq	fr	gs	fs	gp	qr
jt	kt	ju	kv	lw	sv	sw	il	iu
ox	oy	xz	qA	zB	my	nB	nA	mq
tC	tD	pE	vF	rG	vG	EF	pC	rD
CH	yI	uz	FJ	wz	yJ	wF	CI	uH
xH	DI	xE	AJ	BG	GJ	BE	AI	DH
C	I	p	A	l	g	n	zwldbox	
H	D	u	q	r	m	h		

References

- [1] D. Archdeacon, The medial graph and voltage-current duality, *Discrete Math.* 104 (1992) 111–141.
- [2] A. Bouchet, Orientable and nonorientable genus of the complete bipartite graph, *J. Combin. Theory Ser. B* 24 (1978) 24–33.
- [3] A. Bouchet, Constructing a covering triangulation by means of a nowhere-0 dual flow, *J. Combin. Theory Ser. B* 32 (1982) 316–325.
- [4] D.L. Craft, Surgical techniques for constructing minimal orientable imbeddings of joins and compositions of graphs, PhD thesis, Western Michigan University, 1991.
- [5] D.L. Craft, On the genus of joins and compositions of graphs, *Discrete Math.* 178 (1998) 25–50.
- [6] M.N. Ellingham, C. Stephens, The nonorientable genus of joins of complete graphs with large edgeless graphs, submitted for publication.
- [7] M.N. Ellingham, C. Stephens, X. Zha, Counterexamples to the nonorientable genus conjecture for complete tripartite graphs, *European J. Combin.* 26 (2005) 387–399.
- [8] P. Franklin, A six colour problem, *J. Math. Phys.* 13 (1934) 363–369.
- [9] J.L. Gross, T.W. Tucker, *Topological Graph Theory*, Wiley Interscience, New York, 1987.
- [10] P.J. Heawood, Map-colour theorem, *Quart. J. Pure Appl. Math.* 24 (1890) 332–338.
- [11] L. Heffter, Über das Problem der Nachbargebiete, *Math. Ann.* 38 (1891) 477–508.
- [12] M. Jungerman, The genus of the symmetric quadripartite graph, *J. Combin. Theory Ser. B* 19 (1975) 181–187.
- [13] M. Jungerman, The nonorientable genus of the symmetric quadripartite graph, *J. Combin. Theory Ser. B* 26 (1979) 154–158.
- [14] K.-i. Kawarabayashi, C. Stephens, X. Zha, Orientable and nonorientable genera of some complete tripartite graphs, *SIAM J. Discrete Math.* 18 (2004) 479–487.
- [15] Z. Magajna, B. Mohar, T. Pisanski, Minimal ordered triangulations of surfaces, *J. Graph Theory* 10 (1986) 451–460.
- [16] B. Mohar, C. Thomassen, *Graphs on Surfaces*, Johns Hopkins University Press, Baltimore, 2001.
- [17] B. Mohar, T.D. Parsons, T. Pisanski, The genus of nearly complete bipartite graphs, *Ars Combin.* 20 (1985) 173–183.
- [18] G. Ringel, Bestimmung der Maximalzahl der Nachbargebiete auf nichtorientierbaren Flächen, *Math. Ann.* 127 (1954) 181–214.
- [19] G. Ringel, Farbensatz für orientierbare Flächen vom Geschlecht $p > 0$, *J. Reine Angew. Math.* 193 (1954) 11–38.
- [20] G. Ringel, Das Geschlecht des vollständigen paaren Graphen, *Abh. Math. Sem. Univ. Hamburg* 28 (1965) 139–150.
- [21] G. Ringel, Der vollständige paare Graph auf nichtorientierbaren Flächen, *J. Reine Angew. Math.* 220 (1965) 88–93.
- [22] G. Ringel, *Map Color Theorem*, Springer, Berlin, 1974.
- [23] G. Ringel, J.W.T. Youngs, Solution of the Heawood map-coloring problem, *Proc. Natl. Acad. Sci. USA* 60 (1968) 438–445.
- [24] G. Ringel, J.W.T. Youngs, Das Geschlecht des symmetrischen vollständigen dreifarbbaren Graphen, *Comment. Math. Helv.* 45 (1970) 152–158.
- [25] S. Stahl, A.T. White, Genus embeddings for some complete tripartite graphs, *Discrete Math.* 14 (1976) 279–296.
- [26] A.T. White, The genus of cartesian products of graphs, PhD thesis, Michigan State University, 1969.
- [27] A.T. White, The genus of the complete tripartite graph $K_{mn,n,n}$, *J. Combin. Theory* 7 (1969) 283–285.